

Shanbara, HK, Ruddock, F and Atherton, W

A viscoplastic model for permanent deformation prediction of reinforced cold mix asphalt

<http://researchonline.ljmu.ac.uk/id/eprint/9084/>

Article

Citation (please note it is advisable to refer to the publisher's version if you intend to cite from this work)

Shanbara, HK, Ruddock, F and Atherton, W (2018) A viscoplastic model for permanent deformation prediction of reinforced cold mix asphalt. Construction and Building Materials, 186. pp. 287-302. ISSN 0950-0618

LJMU has developed **LJMU Research Online** for users to access the research output of the University more effectively. Copyright © and Moral Rights for the papers on this site are retained by the individual authors and/or other copyright owners. Users may download and/or print one copy of any article(s) in LJMU Research Online to facilitate their private study or for non-commercial research. You may not engage in further distribution of the material or use it for any profit-making activities or any commercial gain.

The version presented here may differ from the published version or from the version of the record. Please see the repository URL above for details on accessing the published version and note that access may require a subscription.

For more information please contact researchonline@ljmu.ac.uk

A viscoplastic model for permanent deformation prediction of reinforced cold mix asphalt

Hayder Kamil Shanbara^{a,c,*}, Felicite Ruddock^b and William Atherton^b

^a Department of Civil Engineering, Faculty of Engineering and Technology, Liverpool John Moores University, Henry Cotton Building, Liverpool L3 2ET, UK

^b Department of Civil Engineering, Faculty of Engineering and Technology, Liverpool John Moores University, Peter Jost Centre, Liverpool L3 3AF, UK

^c Civil Engineering Department, College of Engineering, Al Muthanna University, Sammawa, Iraq

*Corresponding author

E-mail address: H.K.Shanbara@2014.ljmu.ac.uk, hayder.shanbara82@gmail.com

Declarations of interest: none

Abstract

A reliable viscoplastic model of natural and synthetic fibres reinforced cold bitumen emulsion mixture is developed and applied to characterize the rutting behaviour of asphalt pavement by using finite element analysis. It is indicated that the traffic load parameters such as temperature, static loading condition and vehicular speed not only affects the rutting depth, it accelerates the rutting rate, causing the pavement earlier enter into rutting failure with shortened service life. Several finite element models (FEM) have been developed to simulate the behaviour of hot mix asphalts (HMAs), but none exists for cold mix asphalt (CMA) reinforced by natural and synthetic fibres. This research presents the first three dimension (3-D), finite element model (FEM) to assess the viscoplastic behaviour of reinforced CMA mixtures. The model is also able to predict rutting (permanent deformation) of asphalt mixtures under different traffic and environmental loadings, traditional HMA used as a comparison. The enhancement of the performance of CMA mixtures against permanent deformation using finite element software (ABAQUS) was validated by comparing the models' predictions with measurements from wheel-tracking tests at different temperatures (45°C and 60°C). A very good level of agreement

was found between the rutting predicted by the model and the experimental test. The results show that the finite element model can successfully predict rutting of flexible pavements under different temperatures and wheel loading conditions. Finally, the natural and synthetic fibres reinforced CMA mixtures are much more effective at resisting permanent deformation damage than conventional cold and hot asphalt mixtures.

Keywords: ABAQUS; cold mix asphalt; finite element model; natural fibre; rutting; synthetic fibre.

1. Introduction

Asphalt or bitumen are widely used in flexible pavements as aggregate binders because of their high adhesion properties. Flexible pavements are subject to cyclic and sometimes excessive loads during their service life [1, 2]. Their surface is also temperature sensitive in terms of high temperature permanent deformation and low temperature cracking [3, 4]. Permanent deformation (rutting) development is one of the major distresses that frequently occurs in flexible pavements due to the non-linear, viscous and plastic behaviours of asphalt mixes [5]. Permanent deformation can be defined as the unrecoverable vertical deformation of pavements under a vehicle wheel path caused by high temperatures and load repetition. Such deformation can be limited to the asphalt surface layers comprising the viscoelastic and viscoplastic properties of asphalt and the plastic characteristics of aggregates [6].

Hot mix asphalt (HMA) is the main source of flexible pavements used in 95% of the world's paved roads [7]. However, this mixture is considered environmentally unfriendly because it needs substantial amounts of energy to heat the aggregate and asphalt producing CO₂ emissions during both production and laying [8, 9]. Nowadays, several flexible pavement design technologies have been invented to eliminate, or reduce, emissions and save energy regarding asphalt paving production [10]. Cold mix asphalt (CMA) is one of these technologies. CMA is defined as a bituminous mixture of aggregates and asphalt emulsion, mixed at ambient

temperature which does not require the same amount of energy to produce the same CO₂ emissions as HMA [11]. However, it has been considered an inferior mix compared to HMA, mainly in terms of its mechanical properties, the extended curing period required to achieve an optimal performance and its weak early life strength [12]. Poor asphalt mix quality and inadequate design may result in an inefficiently designed layer.

Some strengthening techniques have been trialed in flexible pavements. The reinforcement of asphalt pavements is one method to improve the performance when pavements do not meet traffic, climate and pavement structural requirements. Fibre reinforcement improves the life of a pavement by increasing resistance to permanent deformation and cracking [13]. The addition of fibres to hot and cold mixes as a reinforcing material, enhances the strength, bonding and durability of such mixes [14]. The modification of asphalt mixtures with additives has also been found to decrease permanent deformation and increase durability [15-18]. Modification of asphalt has gained the attention because of its better performance and considered a more economical option compared with neat asphalt binder based on life cycle cost [19].

Flexible pavement responses to traffic loadings are mainly affected by the properties of the materials [20]. A variety of three-dimensional (3-D), finite element simulations have been developed to analyse the responses of flexible pavements [21-26]. The strain experienced by asphalt mixtures under wheel loads has recoverable components (elastic and viscoelastic) and irrecoverable components (plastic and viscoplastic) [27]. Elastic and viscoelastic responses are seen at low traffic volume and low temperatures, while plastic and viscoplastic responses at high traffic volume and high temperatures. Selecting an appropriate constitutive law that takes into account asphalt mixtures' creep behaviour and calibration its parameters using creep testing is important to simulate permanent deformation of flexible pavements by finite element modelling [6]. Picoux, et al. [28] simulated the distribution of vertical deformation to a flexible pavement, subjected to different wheel loadings based on viscoelastic deformation theory.

Dave, et al. [29] developed viscoelastic models to analyse the response of asphalt overlay using thermomechanical impact under different combinations of loading time and temperature. Kai and Fang [30] conducted a 3-D, finite element model of asphalt pavements based on the elastic half-space theory, again examining the effect of load and temperature. Xue, et al. [31] developed a dynamic model to describe the settlement of the surface of asphalt pavements under different temperatures. Pérez, et al. [32] simulated a nonlinear, elasto-plastic Mohr-Coulomb numerical model for recycled flexible pavements, to determine the response of these pavements under two different loads and four types of soil subgrade. Gu, et al. [33] evaluated the effect of geogrid-reinforced flexible pavements by developing two pairs of geogrid-reinforced and unreinforced pavement models. Finite element modeling revealed that rutting resistance is better in the geogrid-reinforced pavement in comparison to the unreinforced pavement.

This research focuses on the evaluation of the response of natural and synthetic fibre reinforced CMA to permanent deformation, using 3-D finite element modelling and experimental tests. The main objectives are to identify the most accurate and effective approach to describe fibre reinforced CMA mixtures using finite element modelling. A 3-D, finite element model is developed and included attention to viscoplastic material behaviours to precisely predict the behaviour of natural and synthetic fibres reinforcement on the development of permanent deformation resistance. Finally, the predicted results from the model are compared with those measured in the lab to identify and verify the applicability of the developed model.

2. Methodology

Firstly, all produced specimens in this research were designed and prepared according to the method that adopted by the Asphalt Institute (Marshall Method for Emulsified Asphalt Aggregate Cold Mixture Design (MS-14)) [34]. After optimizing the emulsion, the length of the fibres and fibre content were determined. Different laboratory tests were used on the

reinforced and unreinforced CMA mixtures to calibrate the parameters of creep power law and to determine the elastic modulus. These tests included the indirect tensile stiffness modulus test and the creep test. A wheel tracking test was also performed to measure the permanent deformation of the mixtures.

A 3-D, finite element model was then developed in ABAQUS with the required test properties. A comparison between measured and predicted results was then carried out to validate the efficiency of the developed model.

3. Viscoplastic behaviour of flexible pavements

Contemporary flexible pavement designs assume that the pavements' response to traffic and environmental stressors is elastic. However, the validity of this assumption is limited to low temperature climate conditions and under rapidly applied vehicle loadings where the deformation to asphalt surfaces is not permanent, returning back to its original shape when the load is removed. At high temperatures, or under slow moving loads, flexible pavements are subject to the type of plastic deformation, which is associated with viscous behaviour. This is the main reason for the development of a new model; to simulate the mechanical response of the new, reinforced, cold mix asphalt and hot mix asphalt. This model is characterized by the elasticity required to simulate the immediate response of the pavement, viscosity to simulate the pavements mechanical response dependent on the strain rate in terms of loading time, and plasticity to simulate plastic flow in terms of permanent deformation.

The viscoplastic deformation of flexible pavements generally depends on the stress level, loading time, number of cycles and temperature. The constitutive law for flexible pavements can be stated as [35]:

$$\varepsilon_{ij} = (\sigma_{ij}, t, N, T) \quad (1)$$

where:

ε_{ij} and σ_{ij} are the strain and stress components, respectively

126 t : time

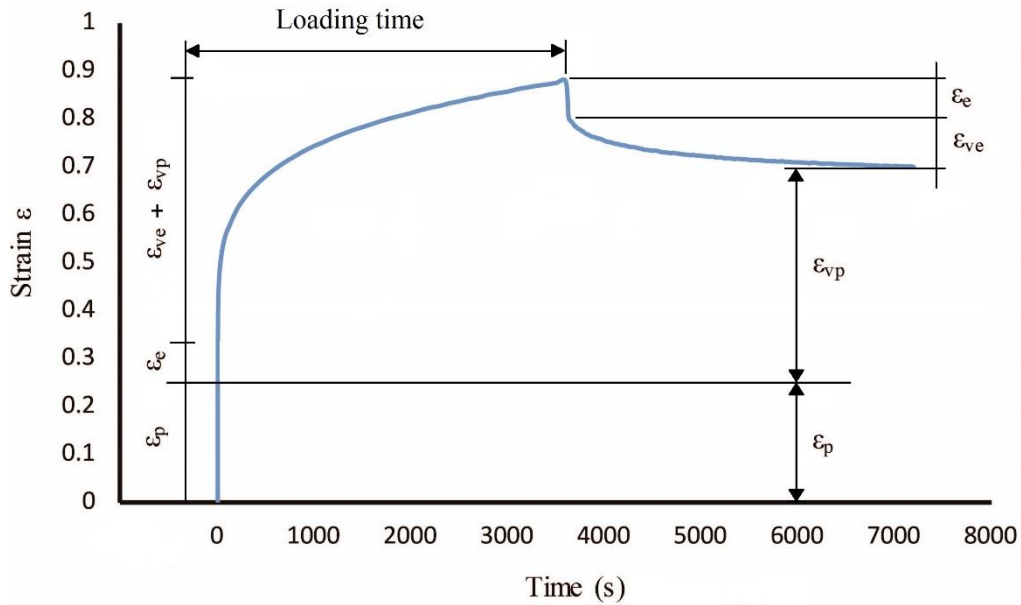
127 N : loading cycles number

128 T : temperature

129 The creep test is used in this research to characterize the viscoplastic behaviour of both the cold
130 and hot asphalt mixes. Four different types of strain develop in flexible pavements when a
131 vehicle moves on the top of them: elastic recoverable strain (ε_e) which is time independent;
132 plastic irrecoverable strain (ε_p) which is time independent; viscoelastic recoverable strain (ε_{ve})
133 which is time dependent, and viscoplastic irrecoverable strain (ε_{vp}) which is time dependent [36,
134 37]. The total strain (ε_t) can be expressed as [35]:

$$\varepsilon_t(\sigma, t, N) = \varepsilon_e(\sigma) + \varepsilon_p(\sigma, N) + \varepsilon_{ve}(\sigma, t) + \varepsilon_{vp}(\sigma, t, N) \quad (2)$$

135 Responses to the above strains can be calculated from the creep test. After applying the load,
136 an instantaneous asphalt mixture response occurs comprising the elastic (ε_e) and plastic (ε_p)
137 strains of the total strain, as shown in



138

139 Figure 1. The elastic strain (ε_e) is the instantaneous reduction at the moment of unloading. The
140 plastic strain (ε_p) can be calculated by subtracting the elastic strain (ε_e) from the instantaneous
141 loading strain ($\varepsilon_e + \varepsilon_p$). The instantaneous loading strain determined from creep curve (for

example Figure 1) when the time is zero. From such creep curves, when the time is just passed zero, the nonlinear part of the curve is started and this point is identified as the cutoff point between the linear and nonlinear parts of creep curves. Both viscoelastic (ϵ_{ve}) and viscoplastic (ϵ_{vp}) strains are time dependent, occurring and overlapping during the loading time stage ($\epsilon_{ve} + \epsilon_{vp}$), as shown in

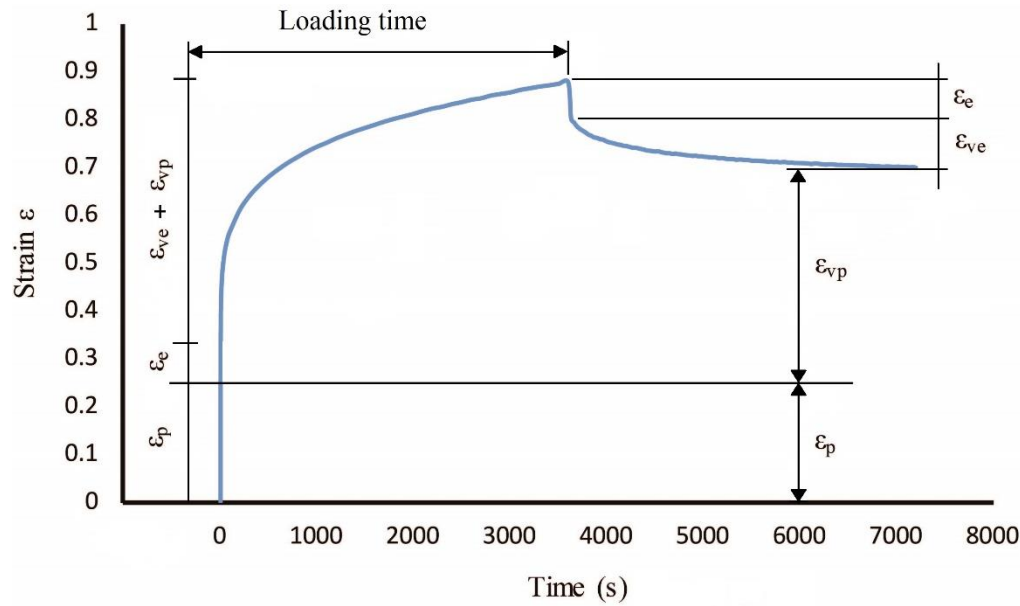


Figure 1. Viscoelastic strain (ϵ_{ve}) is the delayed response during the unloading stage and can be determined as the following:

1. The total strain at time 3600s is ($\epsilon_e + \epsilon_p + \epsilon_{ve} + \epsilon_{vp}$) as can be determined from the creep curve.
2. After the unloading period (3600s) the permanent strain is ($\epsilon_p + \epsilon_{vp}$) as can be determined from creep curve when the time is 7200s.
3. After subtracting the permanent strain from the total strain, elastic (ϵ_e) and viscoelastic (ϵ_{ve}) can be determined ($\epsilon_e + \epsilon_{ve}$).
4. The instantaneous recovery strain after removing loads (at time 3600s) is the elastic strain (ϵ_e) which can be determined from the creep curve.

5. By subtracting the elastic strain (ϵ_e) from the strain that determined in step (3), the viscoelastic strain (ϵ_{ve}) can be determined.

The viscoplastic strain (ϵ_{vp}) can be determined by subtracting the elastic, plastic and viscoelastic strains from the total strain as shown below:

$$\epsilon_{vp} = \epsilon_t - \epsilon_e - \epsilon_p - \epsilon_{ve} \quad (3)$$

As the determined strains in the above are only for one cycle, that means the permanent deformation can be determined. After several cycles, the accumulative permanent deformation can be determined according to how many cycles are applied.

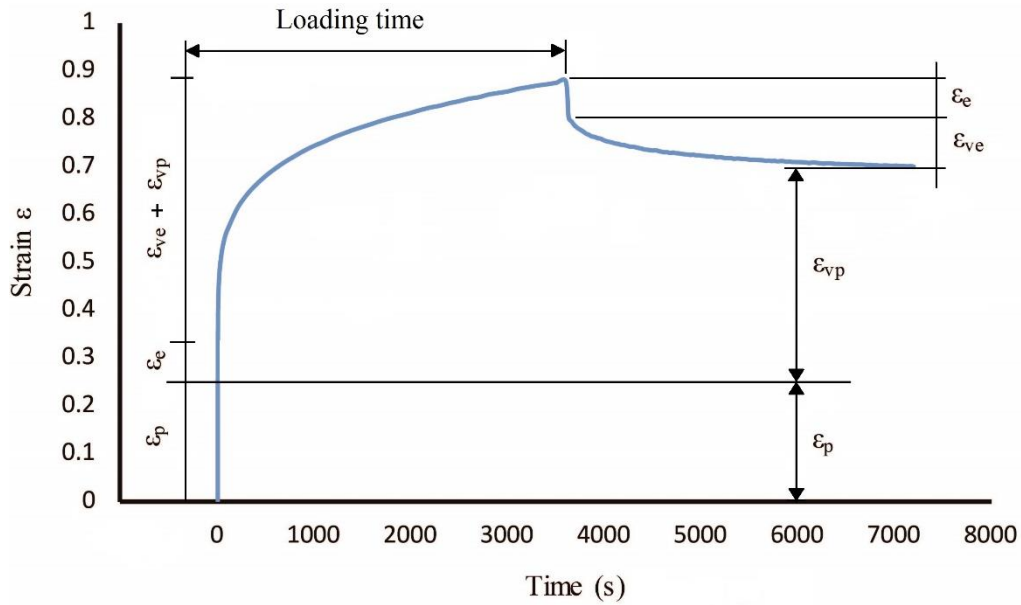


Figure 1. Elastic, plastic, viscoelastic and viscoplastic strains of CMA at 100 kPa and 45°C

Figure 2 illustrates the plastic and viscoplastic strains in the cold mix asphalt at 45°C. From this Figure, it can be seen that the cumulative viscoplastic strain curve increases with a constant steep slope, specifically after 1000 seconds, while the plastic strain curve flattens horizontally with a constant value, as it is a time independent component. This indicates that the irrecoverable deformation of asphalt mixtures in the creep test, mainly depends on the viscoplastic strain component; plastic strain can be considered insignificant if loading occurs over a long time. This confirms the observations by Huang [38].

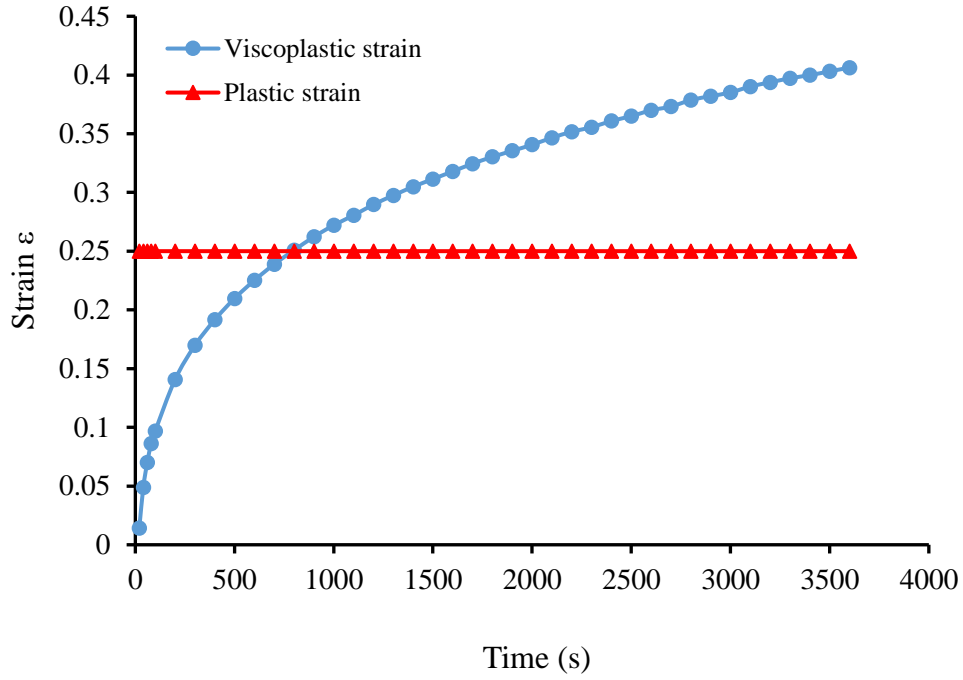


Figure 2. Plastic and viscoplastic strains in the CMA at 100 kPa and 45°C

A viscoplastic model of time-hardening is available in ABAQUS, using the creep power law to represent the nonlinear behaviour of asphalt mixtures. Equation 4 is expressed in a power law form and used to define the creep model [39]:

$$\varepsilon_{vp} = A\sigma^n t^m \quad (4)$$

where A , n and m are the creep power law parameters that relate to the material properties. These parameters depend on bitumen viscosity, aggregate maximum size and aggregate angularity [6]. In this research, the values of the parameters for the conventional CMA and HMA, and the reinforced CMA mixtures were determined according to the results obtained from the creep test. It should be noted that if the creep power law is used to model the time-related behaviour of materials, repeated and continuous loadings result in the same estimation of creep strain on the condition that the total loading periods are the same [6].

4. Methods and experimental procedures

4.1 Materials

4.1.1 Virgin aggregate

The aggregate used in this research for producing asphalt concrete (AC) was crushed granite, which was obtained from Bardon Quarry, Leicestershire, UK. This aggregate was graded using asphalt concrete 14 mm, a close graded surface course in accordance with BS EN 933-1 [40], as presented in Table 1. Based on this, the selected aggregate is one of the most common aggregates used in the production of asphalt, considered hard, durable and clean, of a suitable shape, providing a good level of skid resistance and resistant to permanent deformation. This grade was selected to ensure an appropriate interlock between the particles in the mixtures.

Table 1. Selected mix gradation

Sieve size (mm)	14	10	6.3	2	1	0.063
Passing (%)	100	80	55	28	20	6

4.1.2 Bitumen emulsion

A commercial cationic slow setting bituminous emulsion (C50B3) with 50% bitumen content was used as a binding agent for manufacturing the CMA mixtures to ensure high adhesion between aggregate particles. This type of emulsion is called Cold Asphalt Binder (CAB 50) based on 40/60 penetration grade base bitumen and is supplied by Jobling Purser, Newcastle, UK. The high stability and high adhesion of this cationic emulsion were the reasons for selection as recommended by the supplier. The relevant properties of the selected bitumen emulsion are shown in Table 2. The bitumen emulsion was kept in air-tight sealed containers stored at room temperature. The bitumen emulsions were stirred well into a homogenous state before using in producing the CMA mixtures.

Table 2. Properties of C50B3 bitumen emulsion

Property	Value	Standard
Type	Cationic	
Appearance	Black to dark brown liquid	
Breaking behaviour	110-195	EN 13075-1
Base bitumen Penetration (0.1 mm)	50	EN 1426
Softening Point (°C)	50	EN 1427
Bitumen content, (%)	50	EN 1428
Viscosity (2mm at 40°C)	15-70	EN 12846
PH	5	
Boiling point, (°C)	100	
Adhesiveness	≥ 90%	EN13614
Relative density at 15 °C, (g/ml)	1.05	
Particle surface electric charge	positive	EN 1430
Density (g/cm ³)	1.016	

4.1.3 Bitumen

A traditional binder, consisting of 100/150 penetration grade bitumen supplied by Jobling Purser, Newcastle, UK, was used for the conventional HMA mixture production. This grade of bitumen was selected because it is commonly used in the UK to manufacture HMA mixtures. According to the British Standard PD 6691:2010 [41], this grade is the preferred grade for the production of HMA, having an AC 14 mm close-graded surface course aggregate gradation. The properties of the bitumen used in this research are presented in Table 3.

Table 3. Properties of 100/150 bitumen used in the study

Property	Value
Appearance	Black
Penetration at 25°C (0.1 mm)	141
Softening Point (°C)	43.5
Kinematic viscosity at 135°C (mPa.s)	179
Density (g/cm ³)	1.02

4.1.4 Water

Tap water was used in this research for all types of CMA mixtures. The water was obtained from the domestic water supply pipe in the Henry Cotton Building at Liverpool John Moores University, UK.

4.1.5 Filler

Conventional limestone dust was used in this research as a natural filler obtained from Francis Flower Ltd, UK. Limestone filler plays a physical role through filling the pores between aggregate particles and improving the backing properties.

4.1.6 Fibres

Two different types of fibres were used in this research as reinforcing materials, including synthetic fibre, which is glass fibre (supplied by the Fibre Technologies International Limited-UK), and natural fibre, which is hemp (supplied by the Wild Fibres-UK). These fibres are always as single (mono) fibres. The physical properties of these fibres are presented in Table 4.

Table 4. Natural and synthetic fibre properties

Items	Fibre type	
	Glass	Hemp
Density (kg/m ³)	1380	1500
Tensile strength (MPa)	1600	900
Diameter (µm)	15-19	17-23
Moisture content (%)	0.5	10

4.2 Specimens preparation

The effects of interaction between the asphalt binder and mineral aggregates and the effect of mixing conditions are considered valuable on the properties of the bituminous mixtures [42]. CMA specimens were prepared according to the Marshall method for emulsified asphalt aggregate cold mixture designs (MS-14), as adopted by the Asphalt Institute [34]. According to this procedure, the optimum pre-wetting water content, optimum total liquid content, optimum residual bitumen contents and optimum emulsion content, were 3%, 15.4%, 6.2% and 12.4%, respectively. These results are comparable to those published by [12, 43, 44]. The fibres were added and blended into the mixtures to improve the mechanical properties. To ensure a

consistent distribution of the fibres, water and emulsion in the mixtures, the aggregate together with the fibres and the pre-wetting water were added and mixed for 1 minute using an electric blender [45]. After that, the bitumen emulsion was added progressively throughout the next 30 seconds of mixing, and the mixing was continued for the next 2 minutes. This process allows for the best fibre distribution in the mixtures [46]. In addition, the mixed specimens were placed in the moulds, and then directly compacted with 100 blows (in terms of Marshall specimens were prepared), 50 on each side of the specimens using standard Marshall Hammer (impact compactor), or compacted using a steel roller compactor (in terms of bituminous slabs were prepared).

Fibre reinforcement of bituminous mixtures is deemed a random, direct inclusion of fibres into the mixture. If the fibres are too long, they might not mix well with other materials because some of the fibres may lump together creating a clumping or balling problem. On the other hand, too short fibres might not perform well as a reinforcing material, serving only as an expensive filler in the mixture. Therefore, it is necessary to optimise fibre's length and content to avoid such problems and to ensure the uniformity of fibre distribution in the mixtures. In this research, in order to find the optimum fibre length and content, fibres of varying lengths (10, 14 and 20 mm) were used according to literatures reported [47]. These lengths were selected based on the aggregate maximum size, where, 10 mm is shorter, 20 mm is longer and 14 mm is the same as the aggregate maximum size. Based on the fibre reinforcing HMA and concrete pavements [13, 45, 47-51], fibre contents of 0.15, 0.25, 0.35, 0.45 and 0.55% of total aggregate weight for all fibre lengths, were included in the CMA mixtures. Based on the results of the ITSM test, an optimised fibre length and content were selected and used for the other experimental tests [52].

HMA specimens were prepared for comparison purposes according to the British Standard [41]. 14 mm close graded surface course was used with (100/150) bitumen grade and according

to the British Standard [41] this grade is the preferred grade for producing HMA with the 14 mm close graded surface course aggregate gradation that been used for producing the CMA mixtures. 5.1% optimum binder content by weight of aggregate was added according to PD 6691 (European Committee for Standardization, 2010b) for the Asphalt Concrete (AC) 14 mm close graded surface course. The HMA mixtures were mixed and compacted at temperature of 160-170°C (in accordance with [53], shall not exceed 180°C).

4.3 Testing program and procedures

The testing program was conducted in two phases. In the first phase, fibres were investigated to establish the optimum fibre length and content. In the second phase, the conventional CMA (CON) and HMA mixtures, and the optimised fibre-reinforced CMA mixtures with two different fibres: glass as a synthetic fibre (GLS) and hemp as a natural fibre (HEM), were researched using different laboratory tests as detailed below.

4.3.1 Indirect tensile stiffness modulus test

The indirect tensile stiffness modulus (ITSM) test is a non-destructive test where cylindrical samples are positioned vertically, a diametrical load then applied. This test is used in the current study to determine the stiffness modulus of the bituminous mixtures. Samples are subject to repeated load pulses, with a rest period, along the vertical diameter of the sample, using two loading strips 12.5 mm in width. Loading is applied in a half sine wave form, the loading time is controlled during the test. The rise-time, measured from when the load pulse commences and the time taken for the applied load to increase from initial contact load to the maximum value, is 124 ± 4 ms. The peak load value is adjusted to achieve a target peak, a transient horizontal deformation of 0.005% of the sample diameter. The applied load is measured using a load cell with an accuracy of 2%, the pulse repetition period 3.0 ± 0.1 s.

In order to determine the stiffness modulus [8, 11, 12, 44, 54-56], all CMA specimens were kept in their mould for one day at room temperature (20°C), this representing the first stage of curing, followed by 14 days of curing which represents the early age of pavement life. During this period and because of the fibres, the average stiffness values increase significantly due to reaching a definitive level. This behaviour is due to the bitumen emulsion emitting volatile components, allowing the CMA mixtures to be cured and reach approximately their final strength [14]. Adopting a normal curing temperature (room temperature) in this study was performed to simulate the production, compaction and placing of such mixtures in field conditions and avoid any premature ageing of the binder [57, 58]. Prior to test, the sample were conditioned at the test temperature at least 4 hours. The testing temperatures were set as 5°C, 20°C, 45°C and 60°C. This test was carried out in accordance with BS EN 12697-26 [59] using a Cooper Research Technology HYD 25 testing apparatus. The stiffness modulus was set at the average value of five tested samples.

4.3.2 Creep test

According to the British Standard [60], this test describes a method for determining the creep parameters of bituminous mixtures by means of uniaxial static creep test with some confinement present. Confinement of the sample is necessary to predict realistic rutting behaviour. In this test, a cylindrical specimen is subjected to a static stress. To achieve a certain confinement, the diameter of the loading plate is taken smaller than that of the sample. Creep curve displays of the cumulative strain, expressed in %, of the specimen as a function of the time of load applications. Generally, the following stages can be distinguished in the creep curve Figure 3.

- Stage 1: the decelerated creep part of the strain curve, where the strain rate decreases with increasing loading time.

- Stage 2: the constant strain rate part of the strain curve, where the strain rate is quasi constant and with a turning point in the strain curve.
- Stage 3: the accelerated creep part of the strain curve, where the strain rate increases with increasing loading time.

Depending on the testing conditions and on the mixture properties, one or more stages might be missing.

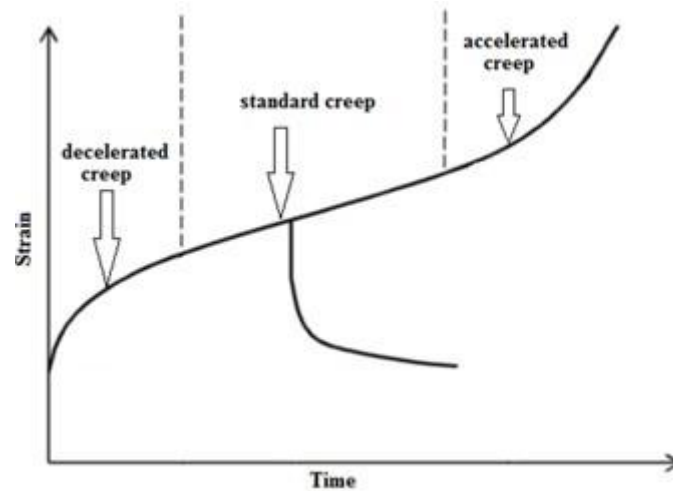


Figure 3. Creep behaviour at constant stress [61]

This test method determines the viscoplastic properties of a cylindrical specimen of bituminous mixture by loading and unloading condition. A cylindrical test specimen with a diameter of 150 mm were prepared and placed between two plan parallel loading plates. The upper plate has a diameter of 100 mm. The specimen is subjected to a static pressure. There is no additional lateral confinement pressure applied. During the test the change in height of the specimen is measured at specified loading time. From this, the cumulative strain (permanent deformation) of the test specimen is determined as a function of the loading time. The results are represented in a creep curve as given in Figure 3. From this, the creep characteristics of the specimen are computed. Prior the test, the specimens were kept at the test temperature within $\pm 1.0^{\circ}\text{C}$ from 4 to 7 hours. To evaluate the viscoplastic characteristics of the bituminous mixtures, creep test

was performed at different testing temperatures (5°C, 20°C, 45°C and 60°C). This test was carried out under 100 kPa stress in accordance with the BS EN 12697-25 [60].

4.3.3 *Wheel tracking test*

Wheel tracking tests were used to measure the rut depth (permanent deformation) of the bituminous mixtures at two different temperatures, 45°C and 60°C. The selection of these two temperatures was based on the British Standard PD 6691:2010 [41]. 45°C represents moderate to heavily stressed sites requiring high rut resistance, while 60°C represents very heavily stressed sites requiring very high rut resistance. Before conducting the tests, an electric blender was used to mix the loose components of the bituminous mixtures. These mixtures then compacted using a steel roller compactor in steel moulds to obtain solid bituminous slabs with dimensions of 40 cm × 30.5 cm × 5 cm, in length, width and thickness respectively.

After compaction, the slab samples were left in their moulds to cure for 24 hours at lab temperature before extraction. Following this, to obtain the final strength of the CMA slabs, the compacted slabs were cured at 40°C for 14 days inside a ventilated oven, then removed and allowed to cool [11, 12, 43, 55, 56, 62, 63]. It is stated that the wheel tracking test should be performed at full curing (at the final mixture strength) because of rutting happen normally at the late ages of the pavements life. In order to prevent the bitumen from ageing, the selected curing temperature (40°C) is less than the bitumen softening point (50°C) [12, 55, 56]. However, curing of such mixtures in the site may take from 2 months to 2 years to obtain the final strength of these mixtures depend on the weather conditions [12, 55, 56].

For the test, a single wheel with a standard vehicle tyre pressure of 0.7 MPa was applied to the surface of the bituminous slab. The wheel was rolled on the surface of the bituminous slab covering a distance of 230 mm at a speed of 42 (±1) times/min (16.1 cm/s) along the centre line of the slab, for 460 minutes (about 20000 wheel load repetitions) under the dry condition. This test was carried out in accordance with BS EN 12697-22 [64].

5. Optimisation of Fibres' Length and Content

Reinforcement can be defined as incorporating materials which have specific properties, within other materials that lack said properties. The primary purpose of fibres as a reinforcing material, is to provide additional tensile and shear strength in the resulting mixtures and then to develop an appropriate amount of strain resistance during the rutting and fatigue process of the mixture [65]. Therefore, optimum fibre's length and content has a major effect on the mixture properties. To obtain the optimum fibres' length and content, natural and synthetic fibres were used in various lengths and contents. The indirect tensile stiffness modulus test was performed in order to conduct fibres' optimisation analysis. Five different fibre contents (0.15%, 0.25%, 0.35%, 0.45% and 0.55%) and three different lengths (10 mm, 14 mm and 20 mm) were carried out to reinforce the CMA mixtures to determine the maximum ITSM. Figure 4 shows the ITSM of all reinforced mixtures with different fibres' length and content. In this Figure, the increase of the ITSM can be observed with increase of fibres content for all fibres length, and then the ITSM decreased with increasing fibres content. Here, 0.35% of fibres content shows the maximum ITSM for all mixtures. The results were in agreement with those found in the literature for example Chen, et al. [45] and Xu, et al. [66] who recommend that 0.3% - 0.4% fibres content as a reinforcing material can provide optimum mechanical properties of bituminous mixtures, based on the results from similar tests. In addition to the fibres content, fibres length was investigated. Figure 4 summarises the results of indirect tensile stiffness modulus test to investigate fibres length effect. The results from the graph show that fibres with 14 mm long have the highest ITSM for the all reinforced CMA mixtures tested. This could be due to the good adherence of the reinforced mixtures with 14 mm fibre length and 0.35% content to the bitumen [13]. According to Li, et al. [67] and Shanbara, et al. [61], shorter and longer fibres than the used aggregate maximum size cannot provide well reinforcing for the bituminous mixtures. Short fibres perform as an expensive filler, while lone fibres tend to lump

together leading to cause balling during the mixing process. This is in agreement with other studies for instance, work by Jeon, et al. [50]. The appropriate fibres length and content provide best placement and distribution into the bituminous mixtures resulting improved interlock between the mixture and fibres [68].

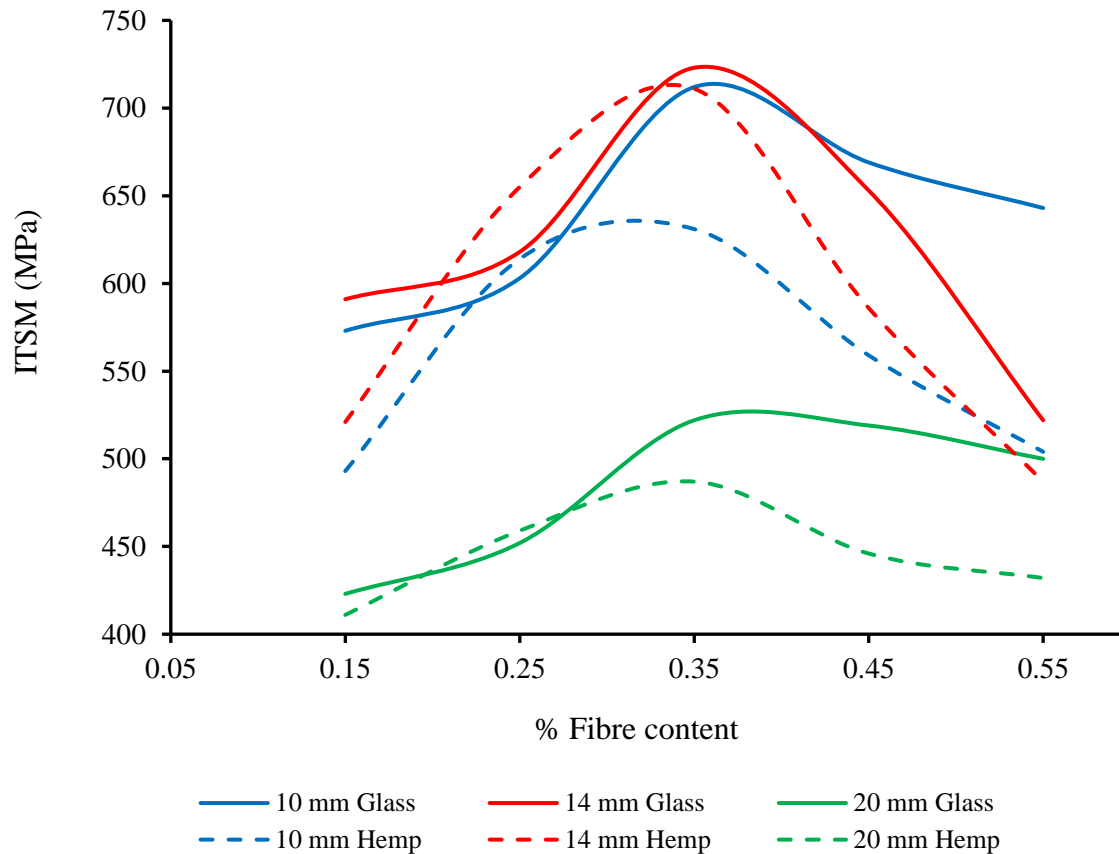


Figure 4. Fibre optimization at 20°C after 2 days

6. Characteristics of the Finite Element Method

The use of the Finite Element Method (FEM) to simulate flexible pavements is currently on the increase because of the nonlinear correlation between stresses and different strain types [3]. Although, 2-D models are acceptable when calculating permanent deformation of flexible pavements, 3-D models are employed to determine more precise and realistic pavement responses [6]. Therefore, in this research, a three-dimensional, finite element analysis of flexible pavement responses under repeated traffic loads, was performed to study the

mechanical properties of the reinforced and unreinforced CMA mixtures. The FEM gives numerical estimations to problems which are too complicated to solve analytically. The problems considered in this model are response to a repeated applied moving load and the viscoplastic material properties of the bituminous mixtures.

The analytic model has a bituminous layer of 400 mm length, 305 mm width and 50 mm thickness, as illustrated in Figure 5. These dimensions were chosen to concur with the wheel tracking test samples which were simulated in this study. During the problem-solving process, displacements of the base layer were restrained in all directions and the layer edges were subject to horizontal restraints. In FEM technique, the body is divided into many small, discrete, finite elements that are solved simultaneously. Simple 3-dimensional, 8-node, linear brick reduced integration elements (C3D8R) were used for all simulations. These finite elements are joined to each other by shared nodes, the combination of nodes and elements forming a mesh. The density of the mesh is dependent on the number of elements used in a particular mesh. The mesh size under the loading area and subject to intense stress and strain, was small (1.5 mm), gradually increasing horizontally to ensure accurate results [69, 70]. Figure 6 shows the finite elements mesh for the model and load distribution on the pavement surface.

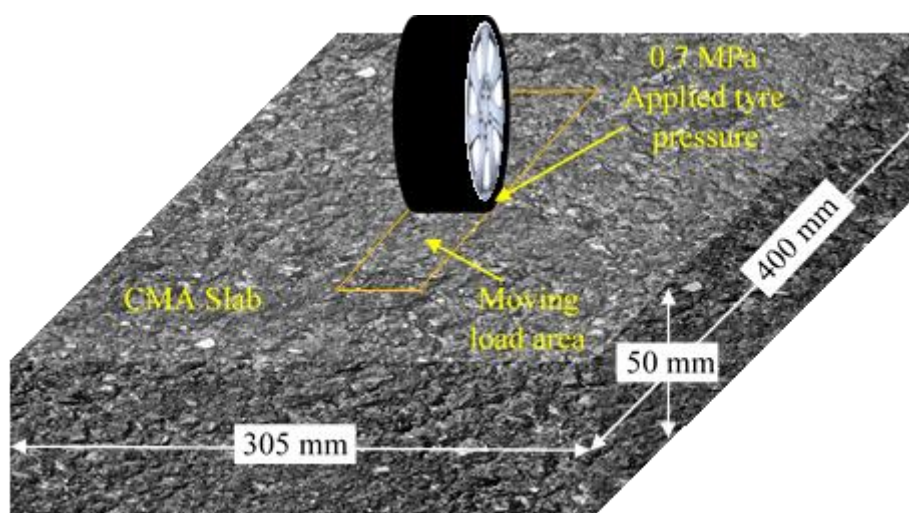


Figure 5. Three-dimensional slab modelling

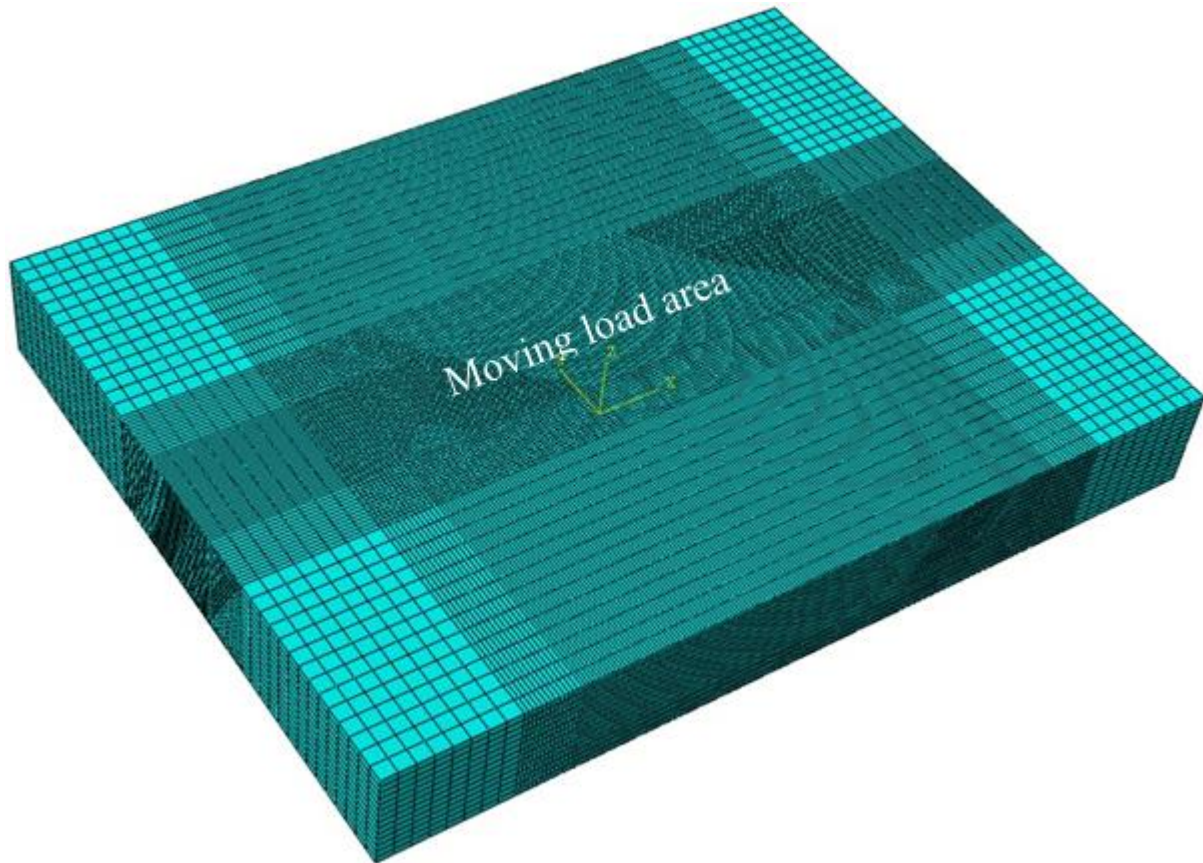


Figure 6. Mesh of the finite element model

In this research, viscoplastic models were developed for the bituminous layers (CMA) containing natural or synthetic fibres as a reinforcing material, and conventional CMA and HMA since the main aim of this research was to qualitatively compare the rutting resistance of different CMA mixtures. Such fibres (glass and hemp) provide random, three-dimensional reinforcement, which improves the tensile and shear strength of the asphalt layer. Four different types of cold and hot mix asphalt mixtures were used in this study: conventional cold (CON) and hot (HMA) mixtures, and reinforced CMA mixtures with glass (GLS) and hemp (HEM). The main variations in the mixtures were the elastic modulus, and creep parameters. It is acknowledged that temperature is an important factor that affects the rutting resistance of all mixtures. With that in mind, the elastic modulus and creep of different mixtures, corresponding to different temperatures, were obtained from the experimental results and a constant Poisson

ratio of 0.35 was assumed. All the flexible pavement material properties for the FEM calculation are presented in Table 5, after 14 days curing for the CMA mixtures.

Table 5. Creep power law and elastic parameters of cold and hot mix asphalt mixtures

Mixture type	Temperature (°C)	A	n	m	E (MPa)
CON	60	1.01×10^{-3}	1.721	-0.0058	35
	45	1.00×10^{-3}	1.648	-0.0011	100
	20	1.91×10^{-3}	1.494	-0.0072	464
	5	9.46×10^{-4}	1.602	-0.0139	581
HMA	60	9.76×10^{-4}	1.756	-0.0093	550
	45	8.19×10^{-4}	1.758	-0.0123	835
	20	6.97×10^{-4}	1.747	-0.0149	1420
	5	5.33×10^{-4}	1.737	-0.0163	4138
GLS	60	6.38×10^{-4}	1.716	-0.0096	604
	45	5.06×10^{-4}	1.721	-0.0137	789
	20	3.23×10^{-4}	1.737	-0.0224	1152
	5	2.17×10^{-4}	1.736	-0.0195	2267
HEM	60	6.81×10^{-4}	1.640	-0.0127	529
	45	5.74×10^{-4}	1.652	-0.0147	713
	20	4.11×10^{-4}	1.668	-0.0152	1100
	5	2.88×10^{-4}	1.655	-0.0149	2047

The creep power law parameters are based on the equation 4, which represents the unloading part of creep test. By fitting the unloading part of the creep curve using Microsoft Excel, the creep power law parameters (A, n and m) are determined. Then these can be used to property the material in ABAQUS. Figure 7 shows an example of fitting the CON creep curve at 20°C.

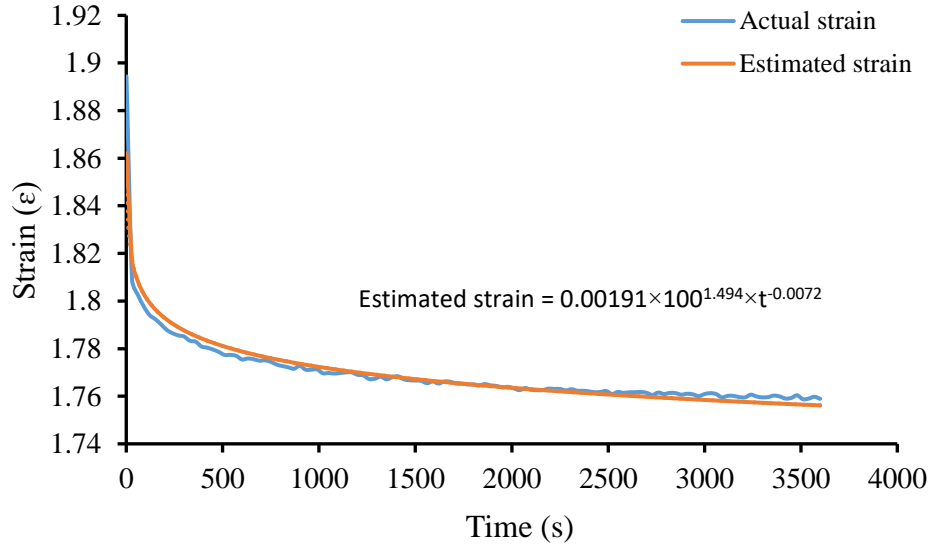


Figure 7. Fitting creep curve of CON at 20°C

A vertical, uniform tyre pressure of 700 kPa was applied as a moving load on the pavement surface having a rectangular loading footprint of 5 cm in length and 3 cm in width, to meet the wheel tracking test requirements. The applied wheel load transfers to the bituminous surface layer through the contact pressure between the tyre and pavement surface. This contact pressure is equal to the pressure from a tyre on a road surface [71], simplified as a rectangular, uniformly distributed, surface load [72, 73]. The moving wheel load zone (Figure 8a) is divided into several small rectangles which have the same width as the tyre footprint (5 cm) and are one-third its length (1 cm). The wheel load occupies three rectangular areas as shown in Figure 8a.

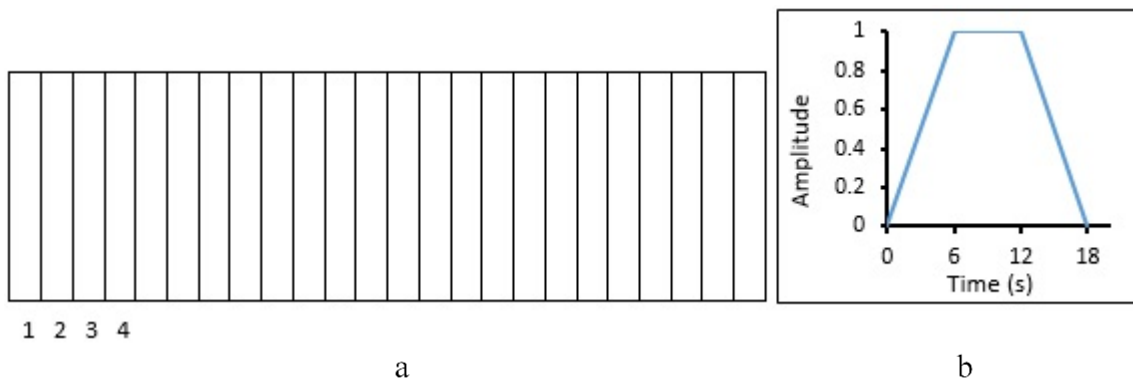


Figure 8. Moving load zone and loading amplitude

When the load gradually moves backwards and forwards, a series of load application steps are performed. At the end of each load application step, the whole load moves forward to a small rectangular area, for example, at the end of the first load application step, the load occupying areas 2, 3 and 4. In order to avoid any impact, load applications on area 4, increase gradually to reach the maximum (700 kPa), at the same time decreasing gradually in area 1, as shown in Figure 8b. Tyre pressure is applied repeatedly on the pavement surface, over a large number of cycles (1.43 s of each cycle), during which the load is applied to each element for 0.18 s to simulate a vehicle speed of approximately 0.6 km/h. The load is then removed as shown in Figure 8b.

7. Validation of the Finite Element Method

In order to validate the finite element model, a validation process was carried out by comparing the experimental results with the finite element modelling output data. A similar set of experiments had been conducted using wheel tracking tests to compare actual rutting (permanent deformation) with the rutting values obtained from the model. The experimental setup comprised an asphalt mix slab with dimensions 5 cm thick, 30.5 cm wide and 40 cm long, over a fixed rigid steel plate. Initially, the slabs were kept in the oven for 14 days at 40°C after compaction, in order to reach the final curing condition stage [11]. During the test, the slabs were subjected to a moving tyre pressure of 700 kPa. The total traveling distance of the tyre on the slab is 23 cm at a speed of 0.6 km/h. Four types of cold and hot asphalt mixtures were prepared to make the slabs. Each type was then wheel track tested at two different temperatures; 45°C and 60°C. The wheel tracking tests were carried out to measure the rut depth on the asphalt pavement surface, along and under the wheel path, after 20000 cycles (28600 s). The rutting value was set at the average value of three tested samples.

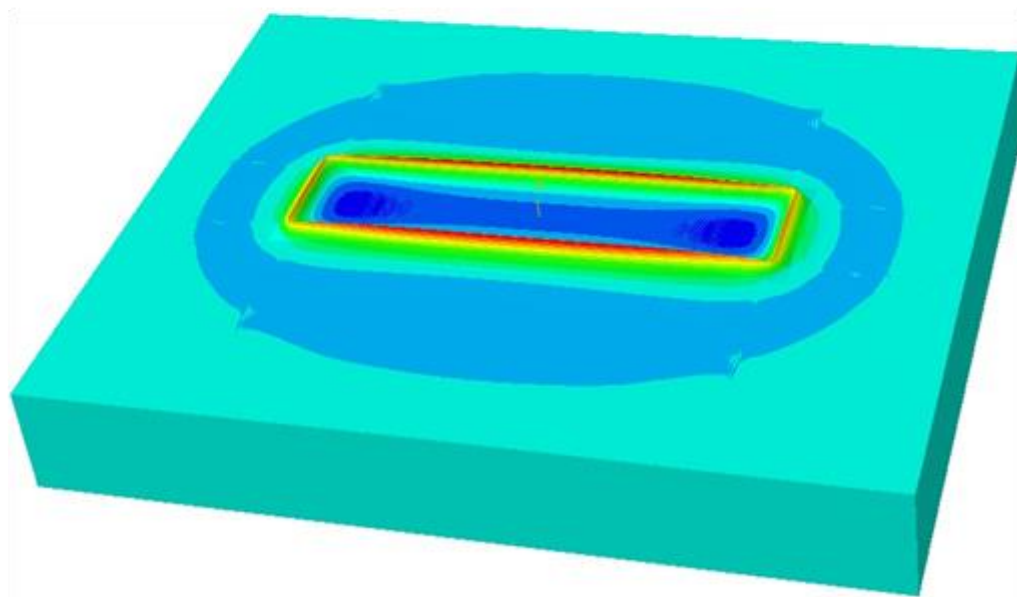
A very slight modification to the model was required to simulate the moving load as it needs to use a repeated moving surface load. The slight modification is, the repeated moving load in

the model was simulated as a surface repeated moving load, while in the wheel tracking test is an actual wheel. All other modelling features remained the same, including loading and unloading time, wheel speed, the total number of load repetitions, boundary conditions and temperature. The total number of load cycles applied on the pavement surface was deemed to be sufficient to distort these pavements. The vertical strain results (rut depth) and the deformation shapes produced on the surface of the asphalt pavement samples using this model, were compared with the pavement strain results which were performed using the wheel tracking test as shown in the Figure 9. Different rut depth measurements were obtained for the HMA and CMA mixtures, at 45°C and 60°C, from the finite element model, to be compared with the experimental data, Figure 10 and 11 presenting these comparisons. It can clearly be seen that there is good agreement on rut depth measurements between the model and the test. The predicted rutting matches well with the measured ruts, even though some variations were observed (between the predicted and measured rutting) between mixture types and temperature. This vibration between the predicted and measured rutting is because of the model assumes that the material properties are uniform and homogenous, whilst in reality the mixtures include some voids and different aggregate interlocks. Also, in reality, the temperature and viscosity of the mixtures can not be distributed equally for the whole mixture and this can not be modelled because of the difficulty of setting different temperatures and viscosities for each particles of the mixture.

It can be also observed from Figure 12 that the transverse rut profile of the experimental results follows the same trend as the slabs that were simulated in the model. Qualitative comparisons of the measured and calculated CMA and HMA responses prove that the finite element model can successfully predict rutting, dependent on the properties of the material, repeated loads and temperatures.

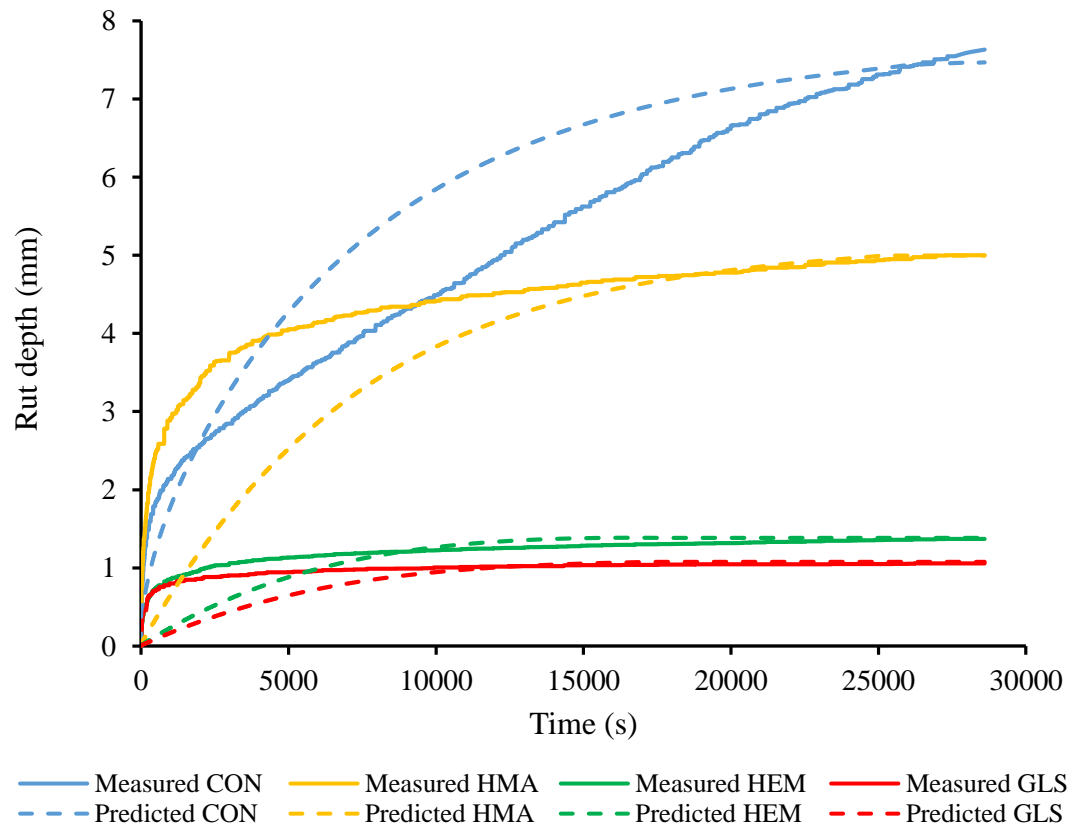
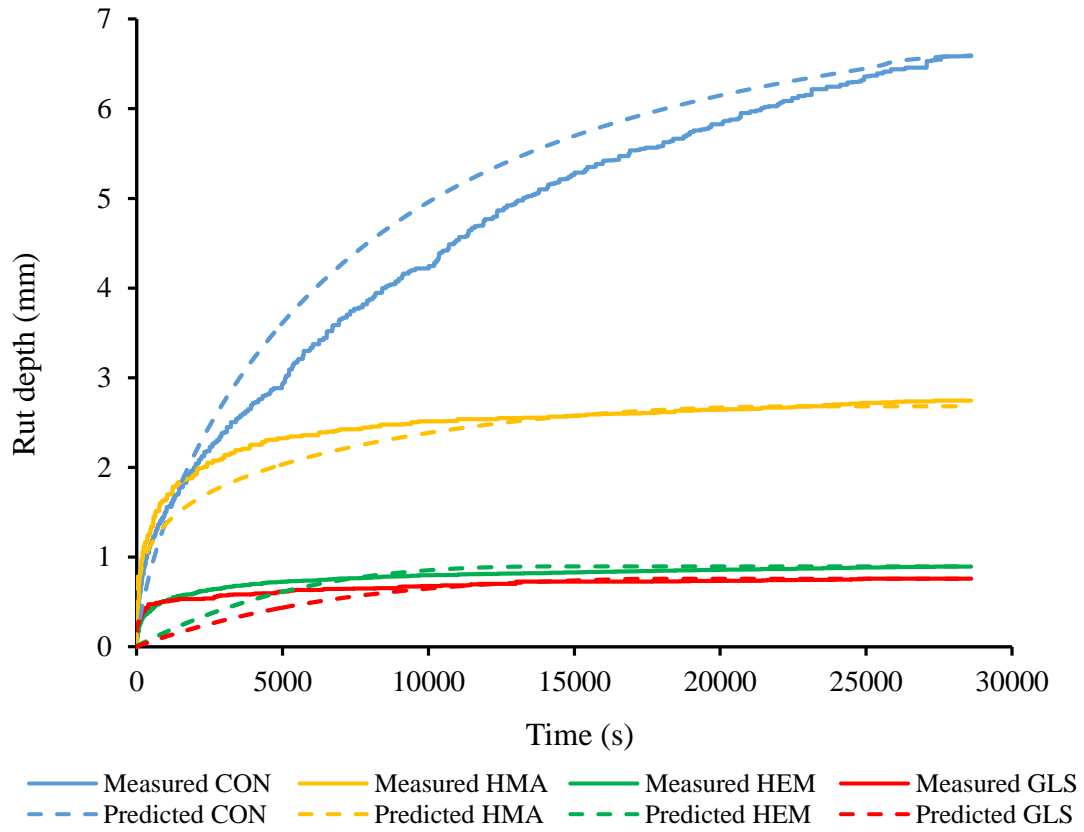


a



b

Figure 9. Conventional CMA deformed shape at 45°C (a) measured, (b) predicted



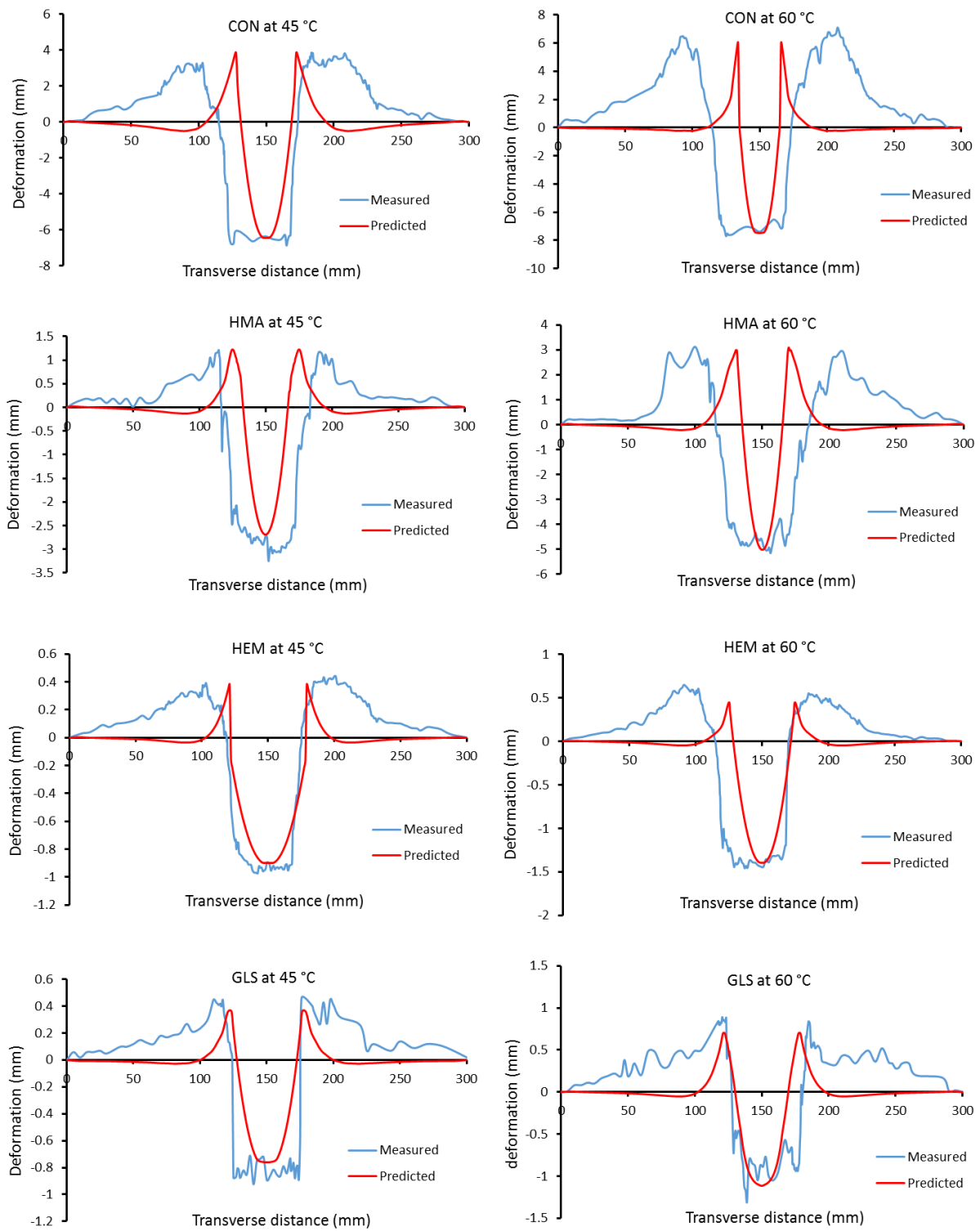


Figure 12. Measured vs. predicted transverse rut profile

8. Parametric study based on the FE model

The validated numerical models presented in Section 7 were used to carry out parametric studies in order to investigate the influence of other parameters on the rutting behaviour of the reinforced and unreinforced CMA mixtures under different loadings and environmental conditions, which were not covered.

8.1 Temperature attributes

To examine the effect of the temperature on the rutting response of the reinforced and unreinforced CMA mixtures using natural and synthetic fibres, two different temperatures were adopted as a moderate to low temperature, i.e. 20°C and 5°C. At low temperatures (about 0°C), rutting resistance increases due to the developed stiffness of the bituminous mixtures in such temperature [67]. Figure 13 and 14 show the rutting variation of the reinforced CMA and conventional CMA and HMA mixtures at different temperatures (20°C and 5°C). As expected from the numerical model, lower rutting of the bituminous mixtures at low temperatures can be observed. Therefore, Flexible pavement design procedures and analysis should consider the actual road pavement temperatures that have an important impact on permanent deformation.

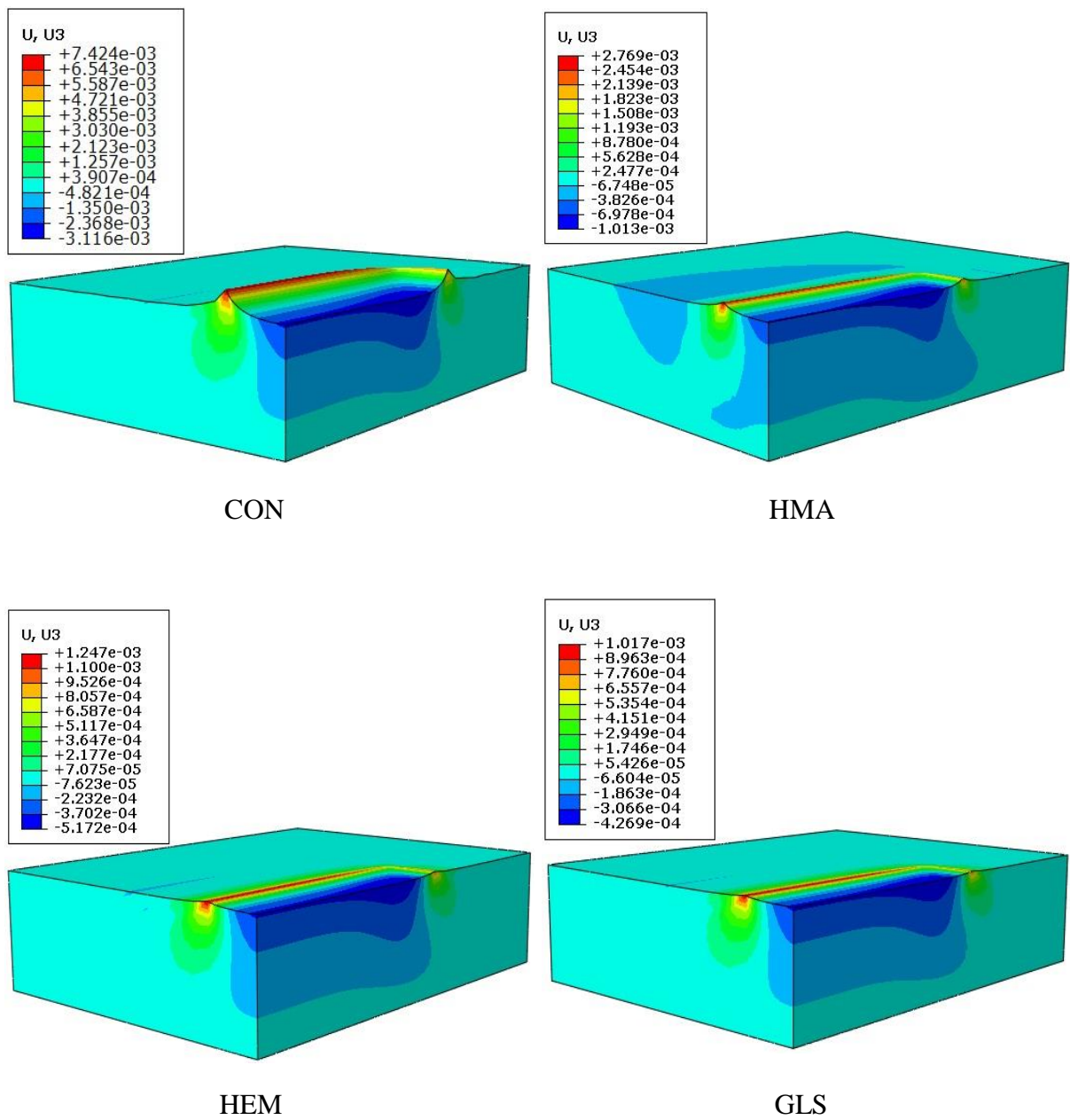


Figure 13. Predicted rutting at 5°C

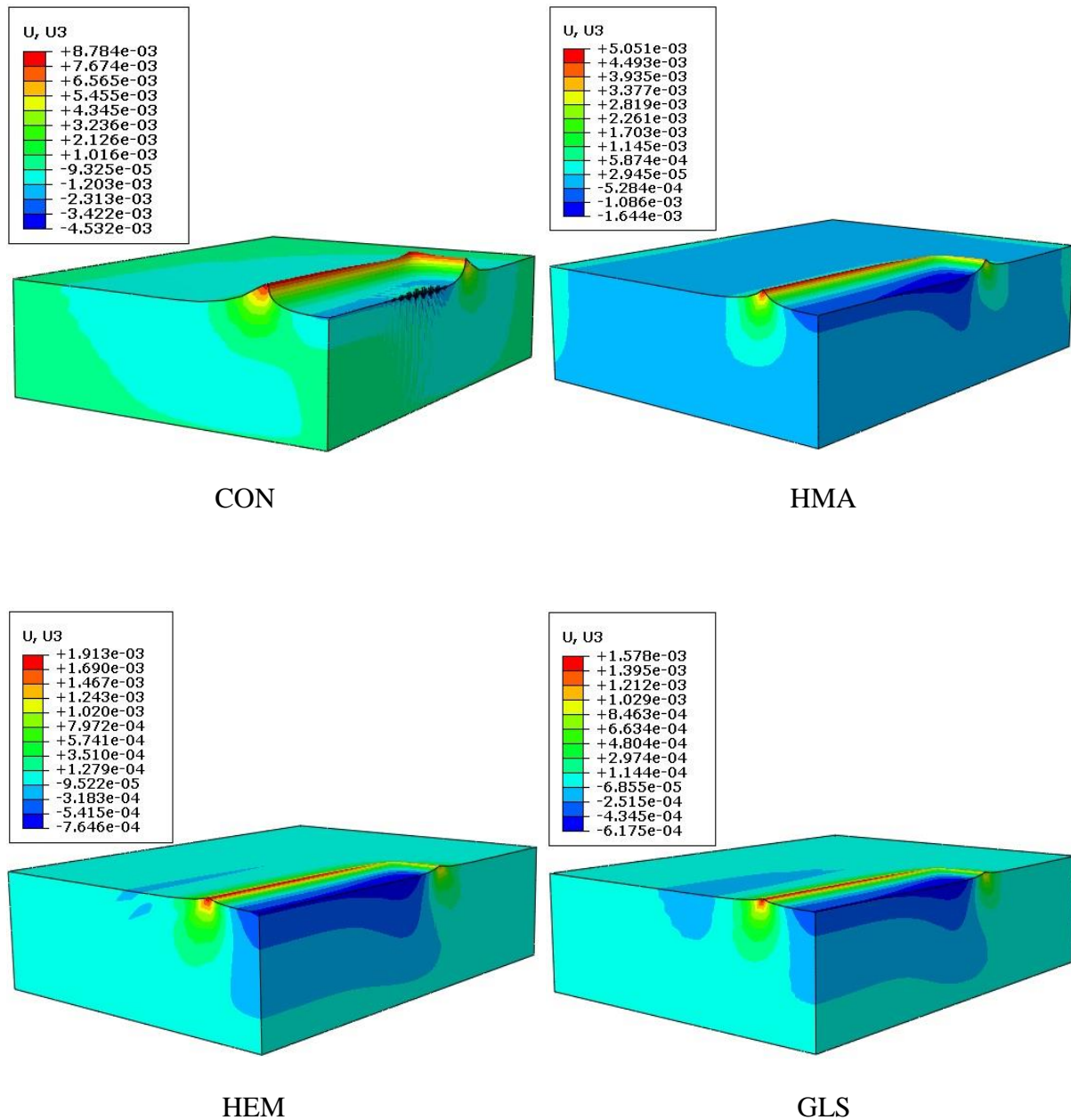
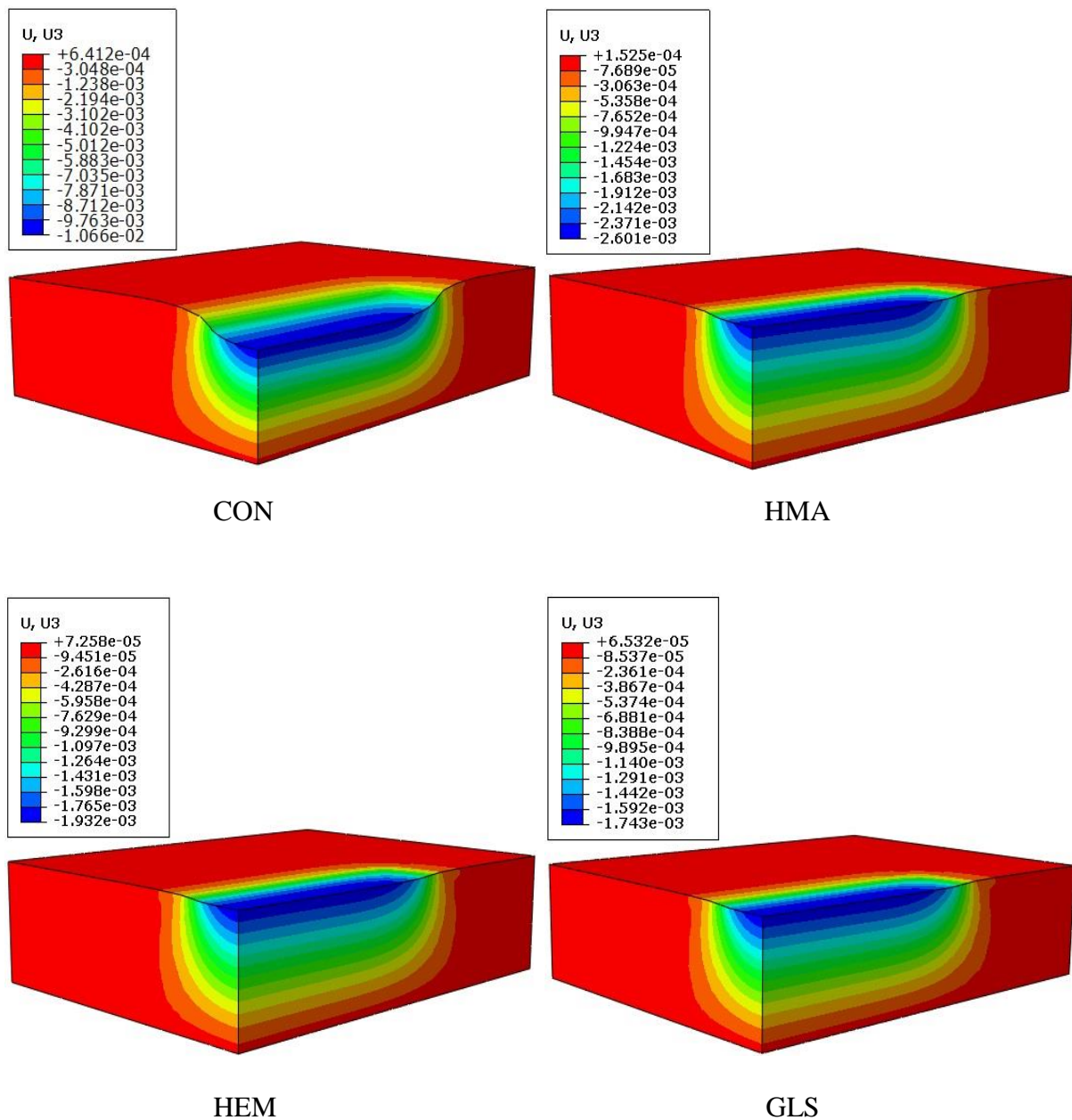


Figure 14. Predicted rutting at 20°C

8.2 Static loading attributes

Rutting of reinforced and unreinforced CMA and HMA mixtures, after 20000 repeated applied moving loads (about 28600 s), were illustrated in Section 7. The rutting of the equivalent static loading condition (20000 s loading) of the same numerical model at four different temperatures is also demonstrated in Figure 15-18. This loading condition was applied resulting permanent deformation that follows the same order of moving loads rutting resistance: the conventional

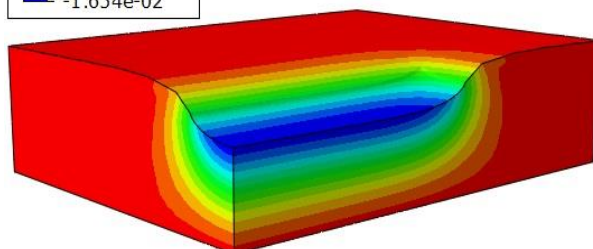
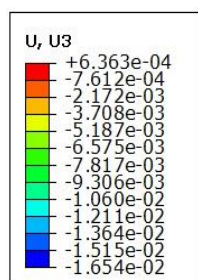
525 CMA and HMA mixtures have the highest rut depth, while the reinforced CMA mixtures with
 526 glass fibre have the shallowest rutting. This is in agreement with Zhi, et al. [74] who reported
 527 that the static loading condition is more damaging to the flexible pavements structure than
 528 moving loads condition. Because there is no rest interval in the static loading condition to allow
 529 bituminous mixtures recover after releasing loads, rutting was greater than that was found in
 530 the moving loading condition [61].



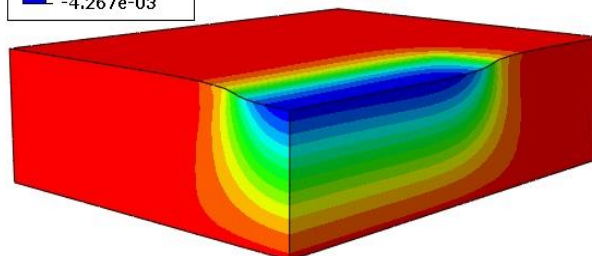
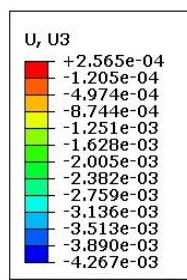
531

532

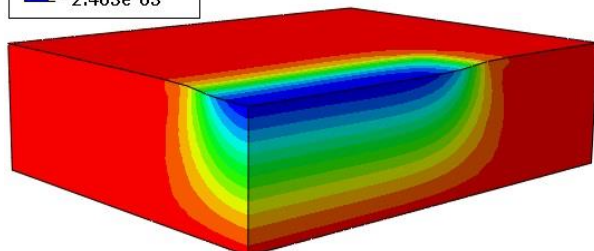
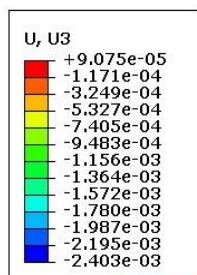
Figure 15. Predicted rutting for static loading at 5°C



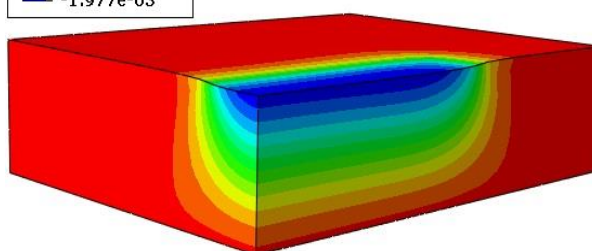
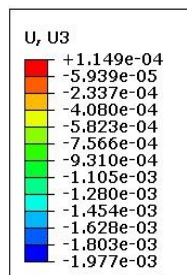
CON



HMA

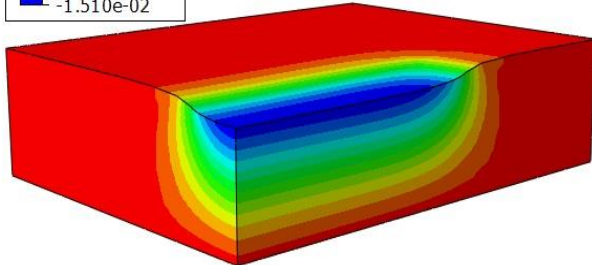
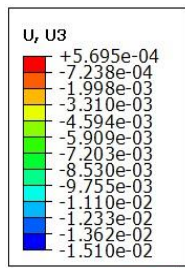


HEM

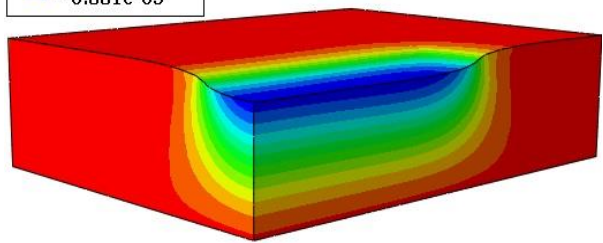
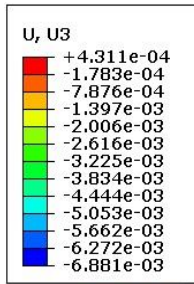


GLS

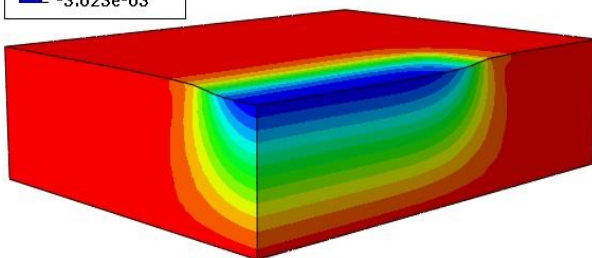
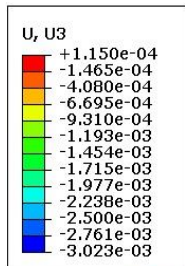
Figure 16. Predicted rutting for static loading at 20°C



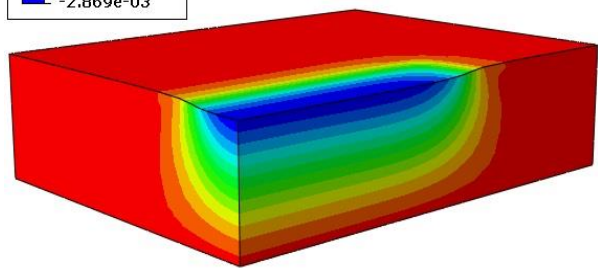
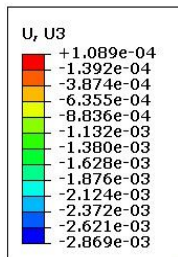
CON



HMA



HEM



GLS

Figure 17. Predicted rutting for static loading at 45°C

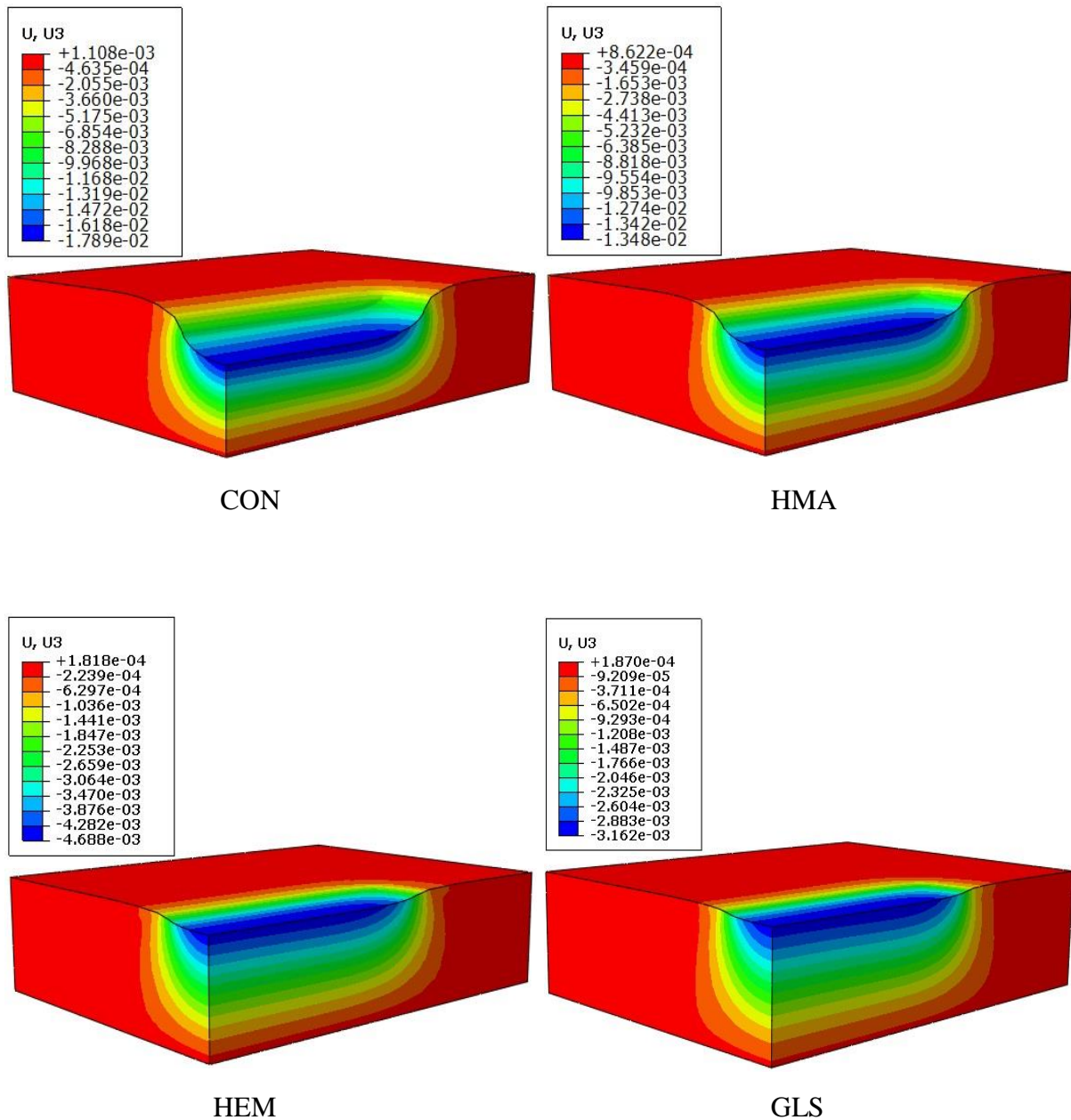


Figure 18. Predicted rutting for static loading at 60°C

8.3 Repeated applied wheel load speed attributes

The influence of the traffic load speeds was performed using the validated numerical model on all cold and hot mixtures with different speeds (5 km/h, 30 km/h and 60 km/h), as shown in Figure 19. At 5 km/h, the cumulative rutting on the bituminous surface layer is significant more than that at 30 km/h, whereas a slight variation in rutting between the 30 km/h and 60 km/h is observed.

The loading time for each repeated wheel pass on each element on the pavement surface, is depending on the moving loads speed. It was 0.0216 s at 5 km/h, 0.0036 s at 30 km/h and 0.0018 s at 60 km/h.

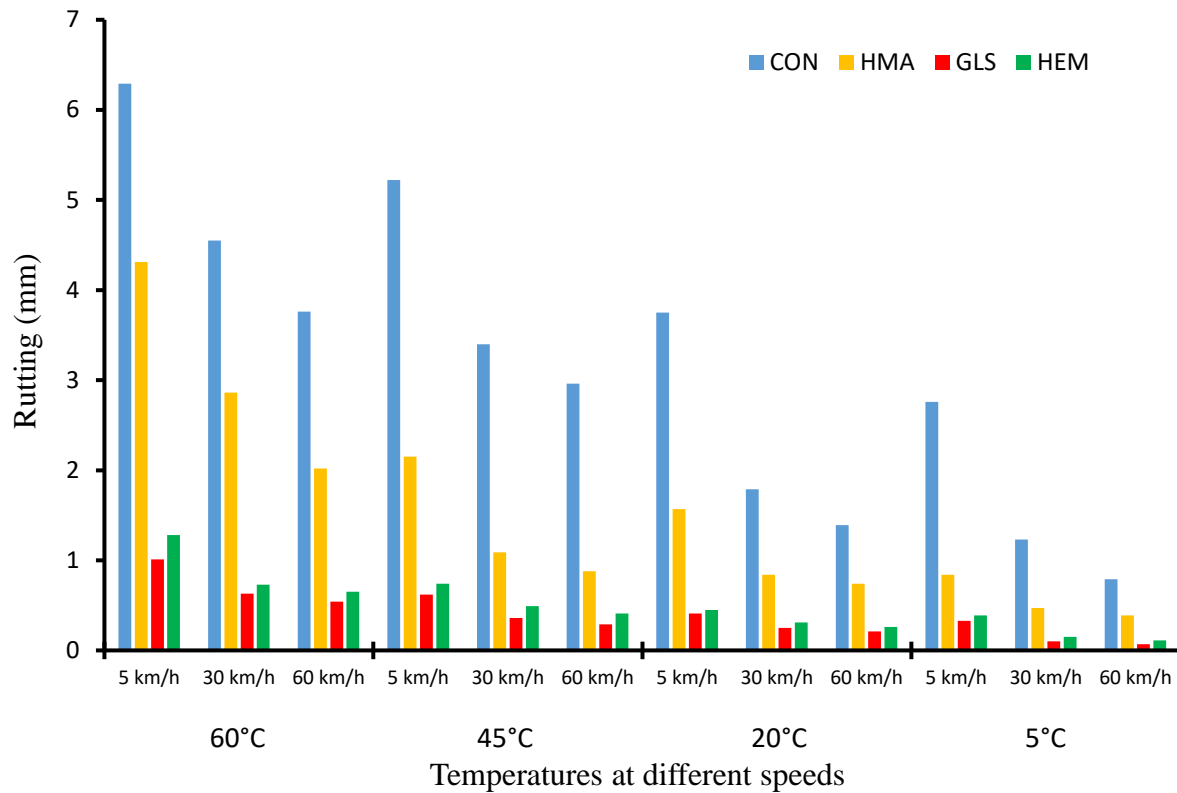


Figure 19. Maximum rut depth for different repeated wheel load speeds after 20000 cycles

8.4 Stress distribution

The validated model in the previous section was used to study the rutting behaviour of the bituminous mixtures in terms of temperature, static loading condition and repeated applied wheel load speed which cannot be obtained from the experimental results. In addition, the model was also used to explain different rutting depth during the repeated moving wheel load on different types of bituminous mixtures. The rutting depth of the reinforced CMA mixtures decreased in comparison to the conventional CMA and HMA mixtures. This reduction is due to the decrease of the pavement stresses at the area underneath the repeated moving load. Figure 20 and 21 show the pattern of stress developed in the all mixtures under repeated moving wheel

load at 5°C and 20°C, if excessive will cause rutting. These Figures show that the maximum stress naturally occurs on the top of the layer under the middle of the wheel path, which might be the main cause of rutting. Stress distribution in the reinforced mixtures is considerably less than stress occurring in the conventional mixtures especially under the moving wheel load.

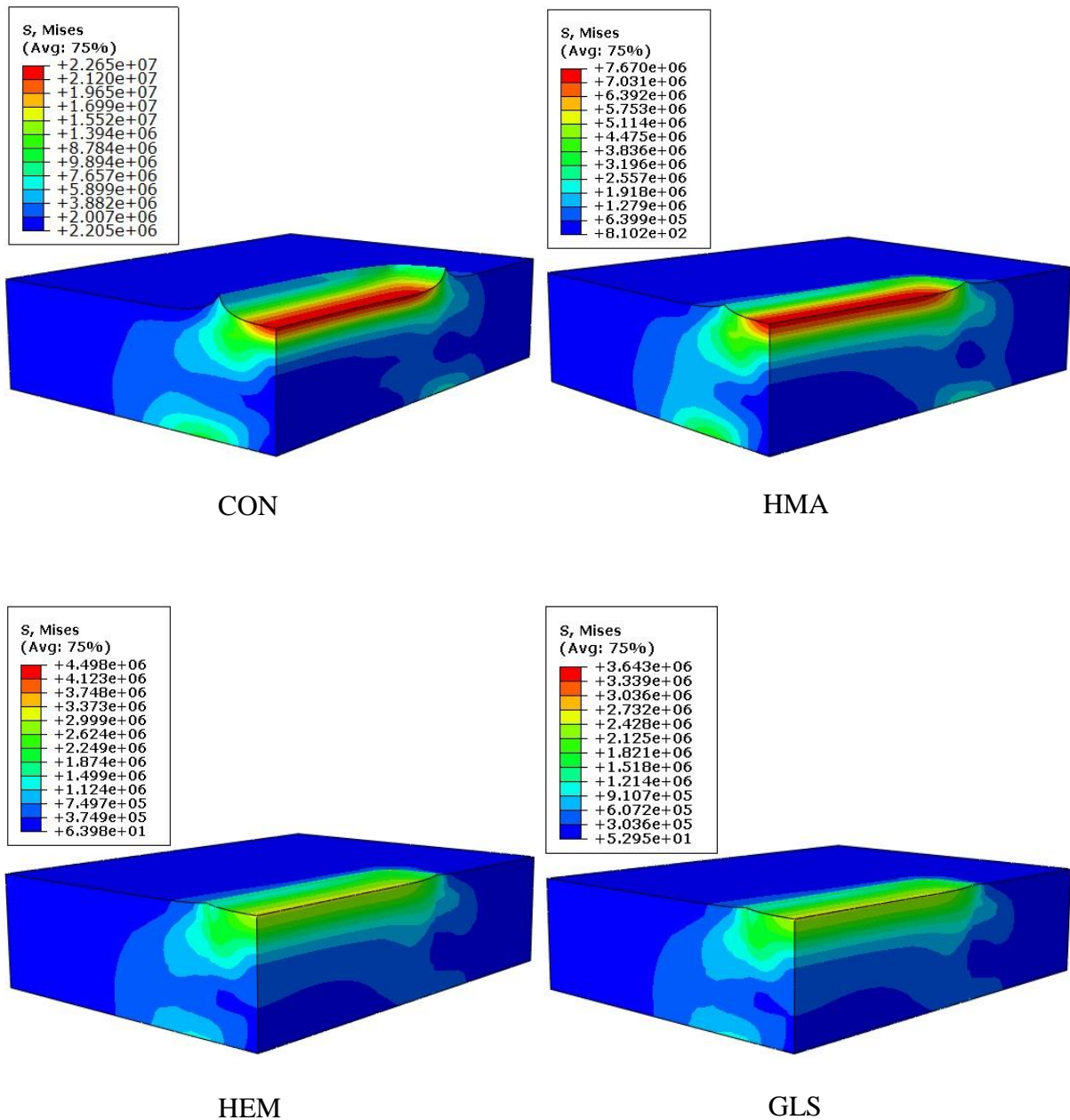


Figure 20. Stress distribution at 5°C

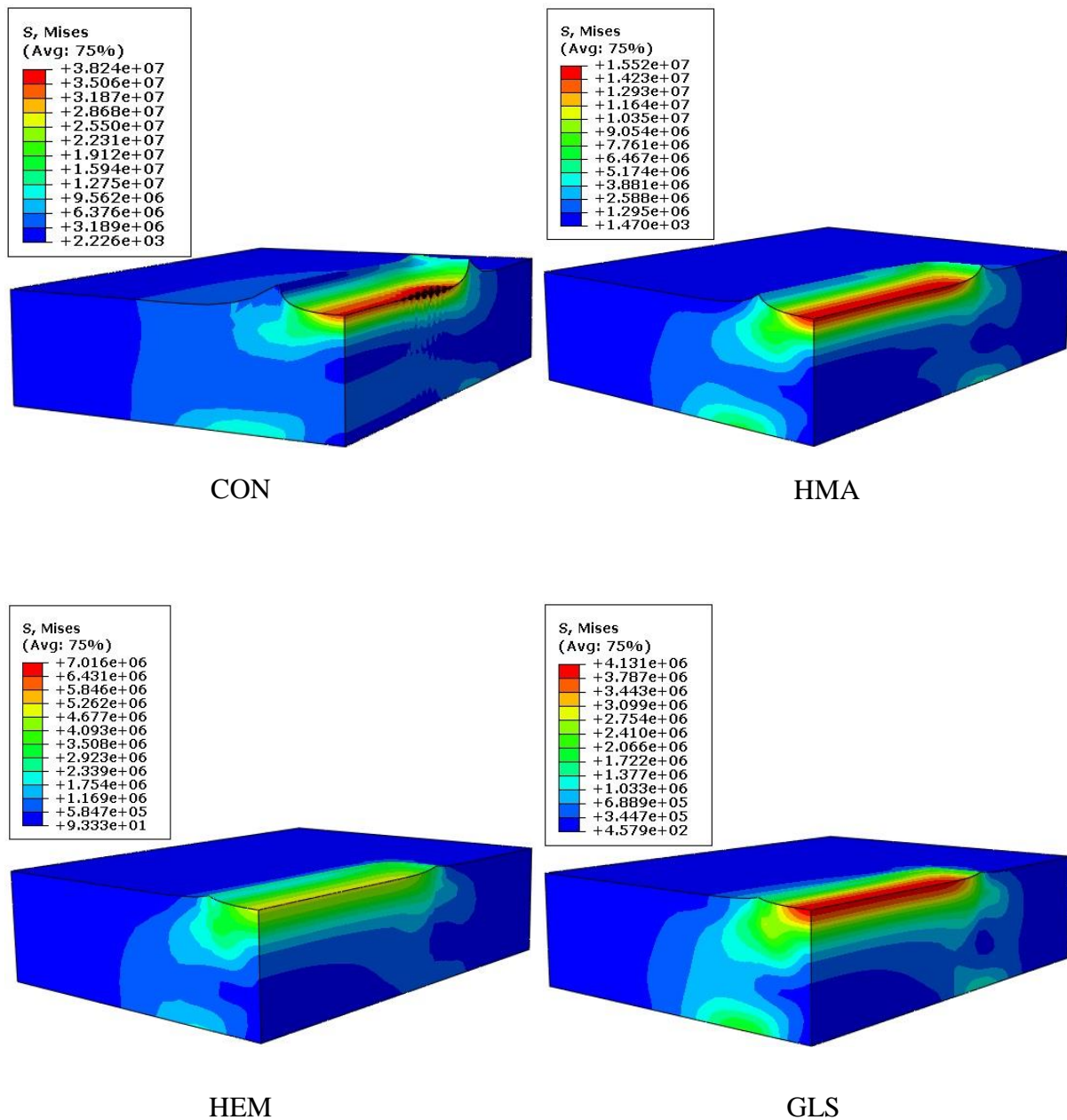


Figure 21. Stress distribution at 20°C

9. Conclusion

In this research, a series of laboratory tests were conducted to characterise permanent deformation characteristics of reinforced CMA mixtures using hemp and glass fibers and also conventional CMA and HMA mixtures. The creep behaviour of such mixtures were investigated based on creep power law parameters. A 3-D viscoplastic model was developed

to simulate a laboratory wheel tracking test. Different types of comparison between the predicted results by the model and those measured using the wheel tracking test were conducted to validate the model. The validated model was finally employed to analyse the influences of different parameters on rutting behaviour that could not be obtained using the laboratory test. The effects of natural and synthetic fibres on these parameters were also considered. The following conclusions were obtained:

- The two reinforced CMA mixtures and the conventional CMA and HMA mixtures exhibited different rutting behaviours under moving and static loading conditions. Their recoverable and irrecoverable deformation trends were well described by the numerical viscoplastic model.
- The addition of hemp and glass fibres to the CMA mixtures as a reinforcing material was found to increase the permanent deformation resistance of such mixtures.
- The results showed the ability of the developed numerical models to predict rutting behaviour under different loading and environment conditions.
- Low and moderate pavement temperatures can effectively improve the resistance to rutting.
- Besides, a comparison between rutting behaviour models under both static and moving loading conditions revealed that the static loading condition exhibits higher rutting than the moving one for all temperatures.
- Effect of low moving load speed on the surface of the road pavements increases rutting effectively, whilst increases rutting slightly at high speeds.

Acknowledgments

This research is a part the first author PhD research Liverpool John Moores University, Faculty of Engineering and Technology, Department of Civil Engineering (Liverpool John Moores

University Reference Number: 669831). The first author would like to express his gratitude to the Ministry of Higher Education & Scientific Research, Iraq and Al Muthanna University, Iraq for financial support under the grant agreement number 29517 dated 17/09/2013. The authors also wish to thank David Jobling-Purser, Steve Joyce, Neil Turner and Richard Lavery for providing the materials for this research project.

References

- [1] Bai, F., Yang, X., and Zeng, G., *A stochastic viscoelastic–viscoplastic constitutive model and its application to crumb rubber modified asphalt mixtures*. Materials & Design, 2016. **89**: p. 802-809.
- [2] Xiao, Y., et al., *Modeling stress path dependency of cyclic plastic strain accumulation of unbound granular materials under moving wheel loads*. Materials & Design, 2018. **137**: p. 9-21.
- [3] Ye, Q., Wu, S., and Li, N., *Investigation of the dynamic and fatigue properties of fiber-modified asphalt mixtures*. International Journal of Fatigue, 2009. **31**(10): p. 1598-1602.
- [4] Al-Hadidy, A.I. and Yi-qiu, T., *Mechanistic approach for polypropylene-modified flexible pavements*. Materials & Design, 2009. **30**(4): p. 1133-1140.
- [5] Safaei, F. and Castorena, C., *Material nonlinearity in asphalt binder fatigue testing and analysis*. Materials & Design, 2017. **133**: p. 376-389.
- [6] Imaninasab, R., Bakhshi, B., and Shirini, B., *Rutting performance of rubberized porous asphalt using Finite Element Method (FEM)*. Construction and Building Materials, 2016. **106**: p. 382-391.
- [7] Arabani, M. and Kamboozia, N., *The linear visco-elastic behaviour of glasphalt mixture under dynamic loading conditions*. Construction and Building Materials, 2013. **41**: p. 594-601.
- [8] Al-Hdabi, A., Al Nageim, H., and Seton, L., *Superior cold rolled asphalt mixtures using supplementary cementations materials*. Construction and Building Materials, 2014. **64**: p. 95-102.
- [9] Yuliestyan, A., et al., *Assessment of modified lignin cationic emulsifier for bitumen emulsions used in road paving*. Materials & Design, 2017. **131**: p. 242-251.

- [10] Jamshidi, A., et al., *Evaluation of sustainable technologies that upgrade the binder performance grade in asphalt pavement construction*. Materials & Design, 2016. **95**: p. 9-20.
- [11] Dulaimi, A., et al., *New developments with cold asphalt concrete binder course mixtures containing binary blended cementitious filler (BBCF)*. Construction and Building Materials, 2016. **124**: p. 414-423.
- [12] Dulaimi, A., et al., *High performance cold asphalt concrete mixture for binder course using alkali-activated binary blended cementitious filler*. Construction and Building Materials, 2017. **141**: p. 160-170.
- [13] Abiola, O.S., et al., *Utilisation of natural fibre as modifier in bituminous mixes: A review*. Construction and Building Materials, 2014. **54**: p. 305-312.
- [14] Ferrotti, G., Pasquini, E., and Canestrari, F., *Experimental characterization of high-performance fiber-reinforced cold mix asphalt mixtures*. Construction and Building Materials, 2014. **57**: p. 117-125.
- [15] Moghaddam, T., B., Karim, M., R., and Abdelaziz, M., *A review on fatigue and rutting performance of asphalt mixes*. Academic Journals, 2011. **6**(4): p. 670-682.
- [16] Vaitkus, A. and Paliukaitė, M., *Evaluation of Time Loading Influence on Asphalt Pavement Rutting*. Procedia Engineering, 2013. **57**: p. 1205-1212.
- [17] Zaumanis, M., Poulikakos, L.D., and Partl, M.N., *Performance-based design of asphalt mixtures and review of key parameters*. Materials & Design, 2018. **141**: p. 185-201.
- [18] Zhang, Y. and Leng, Z., *Quantification of bituminous mortar ageing and its application in ravelling evaluation of porous asphalt wearing courses*. Materials & Design, 2017. **119**: p. 1-11.
- [19] Tan, Y., et al., *Performance optimization of composite modified asphalt sealant based on rheological behavior*. Construction and Building Materials, 2013. **47**: p. 799-805.
- [20] Chen, X., Zhang, J., and Wang, X., *Full-scale field testing on a highway composite pavement dynamic responses*. Transportation Geotechnics, 2015. **4**: p. 13-27.
- [21] Hu, X. and Walubita, L., F., *Effects of Layer Interfacial Bonding Conditions on the Mechanistic Responses in Asphalt Pavements*. JOURNAL OF TRANSPORTATION ENGINEERING, 2011. **137**(1): p. 28-36.

- 650 [22] Kim, H. and Buttlar, W.G., *Finite element cohesive fracture modeling of airport pavements at*
651 *low temperatures*. Cold Regions Science and Technology, 2009. **57**(2-3): p. 123-130.
- 652 [23] Chazallon, C., et al., *Modelling of rutting of two flexible pavements with the shakedown theory*
653 *and the finite element method*. Computers and Geotechnics, 2009. **36**(5): p. 798-809.
- 654 [24] Ameri, M., et al., *Cracked asphalt pavement under traffic loading – A 3D finite element analysis*.
655 Engineering Fracture Mechanics, 2011. **78**(8): p. 1817-1826.
- 656 [25] Ghauch, Z.G. and Abou-Jaoude, G.G., *Strain response of hot-mix asphalt overlays in jointed*
657 *plain concrete pavements due to reflective cracking*. Computers & Structures, 2013. **124**: p. 38-46.
- 658 [26] Li, C. and Li, L., *Criteria for controlling rutting of asphalt concrete materials in sloped*
659 *pavement*. Construction and Building Materials, 2012. **35**: p. 330-339.
- 660 [27] Littel, D., N., Bhasin, A., and Allen, D., H., *Modeling and Design of Flexible Pavements and*
661 *Materials*. 2017, Switzerland: Springer.
- 662 [28] Picoux, B., El Ayadi, A., and Petit, C., *Dynamic response of a flexible pavement submitted by*
663 *impulsive loading*. Soil Dynamics and Earthquake Engineering, 2009. **29**(5): p. 845-854.
- 664 [29] Dave, E., V., et al. *Graded Viscoelastic Approach for Modeling Asphalt Concrete Pavements*,
665 *in: Proceedings of the Multiscale and Functionally Graded Materials Conference, O’Ahu, Hawaii*
666 *(2006)*.
- 667 [30] Kai, L. and Fang, W., *Computer Modeling Mechanical Analysis for Asphalt Overlay under*
668 *Coupling Action of Temperature and Loads*. Procedia Engineering, 2011. **15**: p. 5338-5342.
- 669 [31] Xue, Q., et al., *Dynamic behavior of asphalt pavement structure under temperature-stress*
670 *coupled loading*. Applied Thermal Engineering, 2013. **53**(1): p. 1-7.
- 671 [32] Pérez, I., Medina, L., and del Val, M.A., *Nonlinear elasto–plastic performance prediction of*
672 *materials stabilized with bitumen emulsion in rural road pavements*. Advances in Engineering Software,
673 2016. **91**: p. 69-79.
- 674 [33] Gu, F., et al., *Numerical modeling of geogrid-reinforced flexible pavement and corresponding*
675 *validation using large-scale tank test*. Construction and Building Materials, 2016. **122**: p. 214-230.
- 676 [34] Asphalt Institute, *Asphalt Cold Mix Manual, Manual Series No. 14(MS-14), third ed., Lexington,*
677 *KY 40512–4052, USA, 1989*.

678 [35] Uzarowski, L., *The Development of Asphalt Mix Creep Parameters and Finite Element*
679 *Modeling of Asphalt Rutting*, in *Civil Engineering*. 2006, Waterloo, Ontario, Canada: Waterloo, Ontario,
680 Canada.

681 [36] Sun, L., *Predictions of rutting on asphalt pavements*, in *Structural Behavior of Asphalt*
682 *Pavements*. 2016. p. 601-648.

683 [37] Chen, F., Balieu, R., and Kringos, N., *Thermodynamics-based finite strain viscoelastic-*
684 *viscoplastic model coupled with damage for asphalt material*. *International Journal of Solids and*
685 *Structures*, 2017. **129**: p. 61-73.

686 [38] Huang, Y.H., *Pavement Analysis and Design*. 2004, United States of America: Pearson
687 Education, Inc.

688 [39] Huang B., Mohammad L.N., and Rasoulion M., *Three-Dimensional Numerical Simulation of*
689 *Asphalt Pavement at Louisiana Accelerated Loading Facility*. 2001, Washington, D.C.: Transportation
690 Research Record, National Research Council.

691 [40] European Committee for Standardization, *BS EN 933-1: Part 1, Tests for geometrical properties*
692 *of aggregates: Determination of particle size distribution — Sieving method*, *British Standards*
693 *Institution, London, UK, 2012*.

694 [41] European Committee for Standardization, *BS EN PD 6691, Guidance on the use of BS EN*
695 *13108 Bituminous mixtures – Material specifications*, *British Standards Institution, London, UK, 2010*.

696 [42] Guo, M., et al., *Investigating the interaction between asphalt binder and fresh and simulated*
697 *RAP aggregate*. *Materials & Design*, 2016. **105**: p. 25-33.

698 [43] Al-Busaltan, S., et al., *Green Bituminous Asphalt relevant for highway and airfield pavement*.
699 *Construction and Building Materials*, 2012. **31**: p. 243-250.

700 [44] Al-Hdabi, A., et al., *Development of Sustainable Cold Rolled Surface Course Asphalt Mixtures*
701 *Using Waste Fly Ash and Silica Fume*. *Journal of Materials in Civil Engineering*, 2014. **26**(3): p. 536-
702 543.

703 [45] Chen, H., et al., *Evaluation and design of fiber-reinforced asphalt mixtures*. *Materials & Design*,
704 2009. **30**(7): p. 2595-2603.

705 [46] Abtahi, S.M., Sheikhzadeh, M., and Hejazi, S.M., *Fiber-reinforced asphalt-concrete – A review.*
706 *Construction and Building Materials*, 2010. **24**(6): p. 871-877.

707 [47] Liu, G., Cheng, W., and Chen, L., *Investigating and optimizing the mix proportion of pumping*
708 *wet-mix shotcrete with polypropylene fiber.* *Construction and Building Materials*, 2017. **150**: p. 14-23.

709 [48] Yang, J.M., Kim, J.K., and Yoo, D.Y., *Effects of amorphous metallic fibers on the properties*
710 *of asphalt concrete.* *Construction and Building Materials*, 2016. **128**: p. 176-184.

711 [49] Xu, Q., Chen, H., and Prozzi, J.A., *Performance of fiber reinforced asphalt concrete under*
712 *environmental temperature and water effects.* *Construction and Building Materials*, 2010. **24**(10): p.
713 2003-2010.

714 [50] Jeon, J., et al., *Polyamide Fiber Reinforced Shotcrete for Tunnel Application.* *Materials*, 2016.
715 **9**(3): p. 163.

716 [51] Hesami, S., Ahmadi, S., and Nematzadeh, M., *Effects of rice husk ash and fiber on mechanical*
717 *properties of pervious concrete pavement.* *Construction and Building Materials*, 2014. **53**: p. 680-691.

718 [52] Fu, Z., et al., *Laboratory evaluation of pavement performance using modified asphalt mixture*
719 *with a new composite reinforcing material.* *International Journal of Pavement Research and Technology*,
720 2017.

721 [53] European Committee for Standardization, *BS EN 12697-13: Part 13, Bituminous mixtures —*
722 *Test methods for hot mix asphalt — Temperature measurement, British Standards Institution, London,*
723 *UK, 2000.*

724 [54] Al-Hdabi, A., Al Nageim, H., and Seton, L., *Performance of gap graded cold asphalt*
725 *containing cement treated filler.* *Construction and Building Materials*, 2014. **69**: p. 362-369.

726 [55] Dulaimi, A., et al., *Laboratory Studies to Examine the Properties of a Novel Cold-Asphalt*
727 *Concrete Binder Course Mixture Containing Binary Blended Cementitious Filler.* *Journal of Materials*
728 *in Civil Engineering*, 2017. **29**(9).

729 [56] Dulaimi, A., et al., *Performance Analysis of a Cold Asphalt Concrete Binder Course*
730 *Containing High-Calcium Fly Ash Utilizing Waste Material.* *Journal of Materials in Civil Engineering*,
731 2017. **29**(7): p. 04017048.

732 [57] Khalid, H.A. and Monney, O.K., *Moisture damage potential of cold asphalt*. International
733 Journal of Pavement Engineering, 2009. **10**(5): p. 311-318.

734 [58] Ojum, C., et al. *An investigation into the effects of accelerated curing on Cold Recycled*
735 *Bituminous Mixes*. in *International Conference on Asphalt Pavements, ISAP*. 2014.

736 [59] European Committee for Standardization, *BS EN 12697-26: Part 26, Bituminous mixtures —*
737 *Test methods for hot mix asphalt: Stiffness*, British Standards Institution, London, UK, 2012.

738 [60] European Committee for Standardization, *BS EN 12697-25: Part 25, Bituminous mixtures —*
739 *Test methods for hot mix asphalt — Cyclic compression test*, British Standards Institution, London, UK,
740 2005.

741 [61] Shanbara, H.K., Ruddock, F., and Atherton, W., *Predicting the rutting behaviour of natural*
742 *fibre-reinforced cold mix asphalt using the finite element method*. Construction and Building Materials,
743 2018. **167**: p. 907-917.

744 [62] Al-Busaltan, S., et al., *Mechanical properties of an upgrading cold-mix asphalt using waste*
745 *materials*. Journal of materials in civil engineering, 2012. **24**(12): p. 1484-1491.

746 [63] Al Nageim, H., et al., *A comparative study for improving the mechanical properties of cold*
747 *bituminous emulsion mixtures with cement and waste materials*. Construction and Building Materials,
748 2012. **36**: p. 743-748.

749 [64] European Committee for Standardization, *BS EN 12697-22: Part 22, Bituminous mixtures —*
750 *Test methods for hot mix asphalt — Wheel tracking*, British Standards Institution, London, UK, 2003.

751 [65] Shanbara, H.K., Ruddock, F., and Atherton, W., *A laboratory study of high-performance cold*
752 *mix asphalt mixtures reinforced with natural and synthetic fibres*. Construction and Building Materials,
753 2018. **172**: p. 166-175.

754 [66] Xu, T., et al., *Evaluation of permanent deformation of asphalt mixtures using different*
755 *laboratory performance tests*. Construction and Building Materials, 2014. **53**: p. 561-567.

756 [67] Li, Y., et al., *Effective temperature for predicting permanent deformation of asphalt pavement*.
757 Construction and Building Materials, 2017. **156**: p. 871-879.

758 [68] Saeid, H., Saeed, A., and Mahdi, N., *Effects of rice husk ash and fiber on mechanical properties*
759 *of pervious concrete pavement*. Construction and Building Materials, 2014. **53**: p. 680-691.

760 [69] Shanbara, H.K., et al. *The Linear Elastic Analysis of Cold Mix Asphalt by Using Finite Element*
761 *Modeling*. in *The Second BUiD Doctoral Research Conference*. 2016. Dubai, United Arab Emirates.

762 [70] Chen, J., et al., *Evaluation of pavement responses and performance with thermal modified*
763 *asphalt mixture*. *Materials & Design*, 2016. **111**: p. 88-97.

764 [71] NATIONAL COOPERATIVE HIGHWAY RESEARCH PROGRAM, *Contributions of*
765 *Pavement Structural Layers to Rutting of Hot Mix Asphalt Pavements*. 2002, TRANSPORTATION
766 RESEARCH BOARD: NATIONAL ACADEMY PRESS, WASHINGTON.

767 [72] Wu, J., Liang, J., and Adhikari, S., *Dynamic response of concrete pavement structure with*
768 *asphalt isolating layer under moving loads*. *Journal of Traffic and Transportation Engineering (English*
769 *Edition)*, 2014. **1**(6): p. 439-447.

770 [73] Huang, C., W., et al., *Three-Dimensional Simulations of Asphalt Pavement Permanent*
771 *Deformation Using a Nonlinear Viscoelastic and Viscoplastic Model*. *JOURNAL OF MATERIALS IN*
772 *CIVIL ENGINEERING*, 2011.

773 [74] Zhi, S., et al., *Evaluation of fatigue crack behavior in asphalt concrete pavements with different*
774 *polymer modifiers*. *Construction and Building Materials*, 2012. **27**(1): p. 117-125.

775